AERODYNAMIC ANALYSIS OF COMPLIANT JOURNAL FOIL BEARINGS

Thesis Submitted in Partial Fulfilment of the Requirements for the Degree of

BACHELOR OF TECHNOLOGY (B. Tech.)

In

MECHANICAL ENGINEERING

By

Shubhendra Nath Saha (109ME0301)

Under The Guidance of

Prof. Suraj Kumar Behera,
National Institute of Technology,
Rourkela, 2009-2013

CERTIFICATE

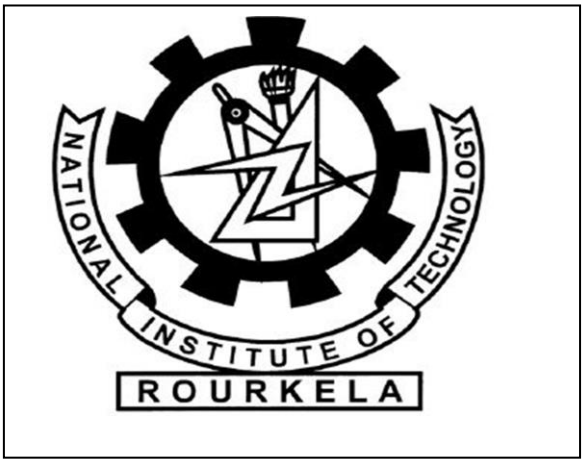

NATIONAL INSTITUTE OF TECHNOLOGY, ROURKELA

This is to certify that this thesis titled by "**Aerodynamic Analysis of Compliant Journal Foil Bearings**'' submitted by **Shubhendra Nath Saha (Roll No. : 109ME0301)** in the partial fulfilment of the requirements for the degree of **Bachelor of Technology** in **Mechanical Engineering, National Institute of Technology, Rourkela**, is an original and authentic work carried out by him under my supervision.

To the best of my knowledge the data or matter used in this thesis has not been submitted to any other University/ Institute for the award of any degree or diploma.

Place: **Prof. Suraj Kumar Behera**

Date: Department of Mechanical Engineering

National Institute of Technology

Rourkela, Osidha

2009-13

ACKNOWLEDGEMENT

It gives me immense pleasure to express my sincere gratitude to my guide Suraj Kumar Behera, Asst. Professor of Department of Mechanical Engineering, National Institute of Technology, Rourkela, Odisha for giving me this wonderful opportunity to work and learn under his able guidance. His invaluable guidance and constant support has made this research possible. I am also indebted for his precious time spent in guiding as well as teaching the fundamentals at each and every stage of this project and also for all the fruitful discussions we had in the past one year.

I would also like to mention a note of thanks for Prof. S.C.Mohanty, Department of Mechanical Engineering, National Institute of Technology, Rourkela for providing me with a Final Year B.Tech. Project in the Design field as well as constantly evaluating our work from time to time during the course of this project. I would also take this opportunity to thank Prof. S.K.Sahoo, Project Coordinator (U.G.) all the other faculties of Department of Mechanical Engineering for their constant support and encouragement.

I would also express my thanks to my friend Mr. D. Jaswant Kumar, another undergraduate project student under my guide for helping to overcome various difficulties which I faced during the coding part of the project.

Finally I would like to express my heartfelt gratitude to my parents and sister for their constant motivation towards successful completion of the project.

SHUBHENDRA NATH SAHA
(109ME0301)
Department of Mechanical Engineering
National Institute of Technology,
Rourkela, Odisha

DATE: 12/5/13
Place: Rourkela

ABSTRACT

This thesis provides a detailed study about the aerodynamic analysis of compliant journal foil bearings. In high speed turbomachinery elements, conventional bearings can't be used since at such a high speed (50000-80000) rpm these bearings get worn and thus they fail. In this project the analysis of a compliant bearing, which has bump foils to enhance the load carrying capacity, has been done. The thin air film between the rotating shaft and the bearing creates the pressure to support the load. Reynolds Equation was first devised for the given compliance system. Due to its nonlinear nature iterative methods are required to solve it. For calculating the pressure distribution and hence the load carrying capacity of the bearings Finite Difference Approximations were used and a unique method, method of quadratic equations was used to find out several parameters. Using MATLAB several codes have been written to find out the pressure profile and the minimum film thickness whose 3 dimensional graphs have been plotted.

After the pressure profile has been generated the load carrying capacity has been evaluated for the bearing under the given input parameters. Thereafter several comparisons have been made between the foil and the rigid bearing on the basis of the plots. Finally two different materials, one used for high temperature applications-Inconel X-750 and another used for low temperature applications Aluminium Bronze have been compared to find out their compatibility in different commercial applications based on their load carrying capacity.

NOMENCLATURE

e	:	Eccentricity of shaft (mm)
Θ,θ	:	Coordinate along the circumferential direction (degrees)
ω	:	Angular speed of rotation (rpm)
ϕ	:	Attitude angle (degrees)
h	:	Fluid film thickness (mm)
W	:	Load carrying capacity (N)
s	:	Bump pitch (mm)
t	:	Thickness of the foil (mm)
l	:	Half bump length (mm)
u	:	Velocity component in x direction (mm/s)
v	:	Velocity component in y direction (mm/s)
w	:	Velocity component in z direction (mm/s)
C	:	Radial clearance (mm)
D	:	Diameter of the shaft (mm)
E	:	Modulus of elasticity (N/mm2)
Le	:	Length of bearing (mm)
R	:	Radius of shaft (mm)
α	:	Compliance Number or Bearing Number of bearing (dimensionless)
υ	:	Poisson's Ratio of Lubricant (dimensionless)
ε_f	:	Eccentricity ratio of bearing (dimensionless)
ρ	:	Density of gas used in bearing (kg/m3
η	:	Coefficient of viscosity of bearing (N-s/mm2)
e_f	:	Eccentricity of foil bearing (mm)
Λ	:	Bearing or compressibility number (dimensionless)
$p_{i,i}$	:	Pressure acting on any node(i,j)
τ	:	Shear stress acting on the control volume (N/mm2)
$\bar{z}$	:	Non dimensional length along z direction (dimensionless)
$\bar{p}$	:	Non dimensional pressure (dimensionless)
$\bar{h}$	:	Non dimensional film thickness (dimensionless)
$\bar{\eta}$	:	Non dimensional coefficient of viscosity (dimensionless)
$\bar{T}$	:	Non dimensional temperature (dimensionless)
p_a	:	Atmospheric pressure (N/mm2)
A, B, C	:	Coefficients of Quadratic Equation (dimensionless)

LIST OF FIGURES

LIST OF TABLES

CONTENTS

CHAPTER-1

INTRODUCTION

Gas bearings have been used to support rotors in machines since the 1960. They have been designed for several applications including gyros, supports for magnetic heads in computer hard disks and special machine tools. Gas bearings enable extremely low frictional torque to be obtained and are used in gyroscopes and other precision instruments.

1.1 USE AND APPLICATIONS

Gas bearings are particularly valuable when they are used to support oil free high speed rotors in precision machines as process gas is used as lubricant. Gas lubricated films are particularly isothermal because the ability of the bearing materials to dissipate heat is greater than the heat generating capacity of gas films which have very low friction losses so no thermal effects appear during gas beating operation. These advantages of gas bearings are due to the fact that the surfaces of journal and bush are separated by a gas (mainly air) layer characterized by a very low (compared with oil) viscosity. Gas bearings retain their advantages at high rotational velocities admissible for oil bearings and rolling bearings.

One of the major problems of developing turbo-expander system for gas liquefaction plants is the instability of the rotor at high rotational speed. For stability of rotor system at high rotational speed, better bearings are required. Gas bearings are one of the solutions of maintaining stability and prevent contamination of working fluids in these plants. Gas bearings of various types can be used in miniature turbines like Aerostatic gas bearings (externally pressurized gas bearings) and Aerodynamic gas bearings (self acting).

The advantages of gas bearings have been full established in the following areas:

- Machine Tools: Use of gas lubrication in grinding spindles allows attainment of high speeds with minimal heat generation.
- Metrology: Air bearings are used for precise linear and rotational indexing without vibration and oil contamination.
- Dental drills: High speed air bearing dental drills are now standard equipment in the profession.

- Airborne air cycle turbo machines: Foil type have been successfully introduced for air cycle turbo machines on passenger aircraft. Increased reliability, leading to reduced maintenance costs, is the benefit derived from air bearings.
- Computer peripheral devices: Air lubrication makes possible high packing density magnetic memory devices, including tapes, disks and drums. Read write heads now operate at sub micro meter operation from the magnetic film with practically no risk of damage due to wear.

1.2 TYPES OF BEARINGS

Gas bearings of categorised into the two following types:

a. Aerostatic bearings (Externally pressurized gas (air) bearings).
b. Aerodynamic bearings. (Self-Acting gas (air) bearings).

AEROSTATIC BEARINGS

Aerostatic Gas Bearings supports its entire designed load at zero speed. This effect results from its principal disadvantage: it requires an external pressure source to create the air film. In principle, gas is supplied to the bearing clearance at a certain gauge pressure. The pressure differential causes the air to flow from the supply point through the bearing gap and out the periphery to atmosphere. The pressure inside the gap creates the load carrying properties which are limited only by the available supply line pressure and material strength. The aerostatic bearing does not suffer from friction induced wear and in addition it has no starting and stopping friction.

AERODYNAMIC/HYDRODYNAMIC GAS BEARINGS

In the case of aerodynamic or self-acting bearings, the air film is created by the relative motion of two mating surfaces separated by a small distance. From rest, as the speed increases, a velocity induced pressure gradient is formed across the clearance. The increased pressure between the surfaces creates the load carrying effect. The load capacity is dependent on the relative speed at which the surface moves and therefore at zero speed, the bearing supports no load. In general, aerodynamic bearings suffer from decreased load carrying capacity. In addition, the zero loads at zero speed effect causes starting and stopping friction

and results in some wearing of the bearing surfaces, however this can be treated with application of film of solid lubricant on the bearing and/or journal surface.

1.3 COMPLIANT JOURNAL BEARINGS

Compliant journal bearings are bearings with compliant bearing surfaces. Foil bearings is a compliant bearing having a unique type of operation with several different kinds of applications. As compared to the conventional rigid bearings they have higher load carrying capacity, better stability as well as greater amount of enduring strength. Moreover these are self-acting bearings and can operate with ambient air or any other gas as the lubricating fluid. Since no hard-core lubrication system is present the result is lesser amount of weight and lower maintenance cost. The most common lubricant used is air since it is abundant in nature and can operate at higher temperatures while oil based lubricants tend to fail at higher temperatures since their viscosity is inversely proportional to rise in temperature.

PHYSICAL LOOK

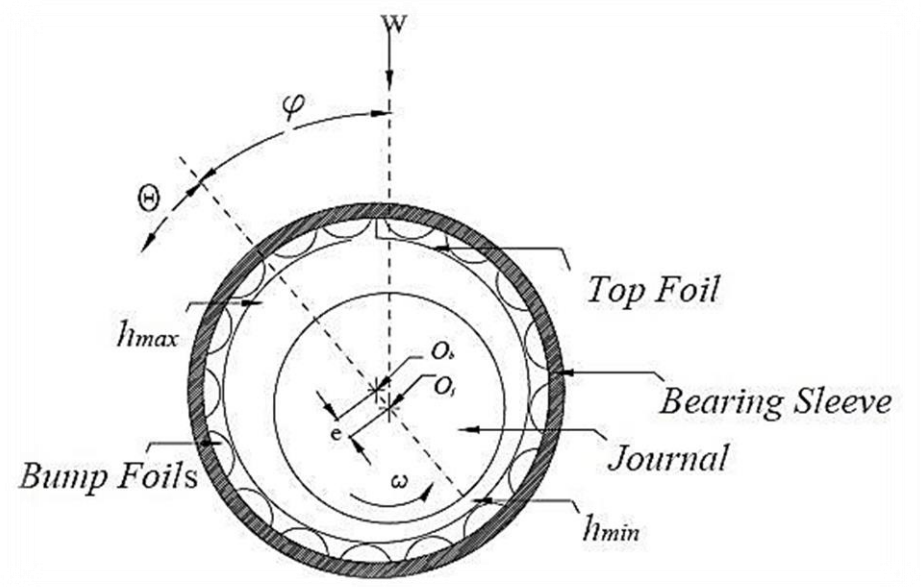

FIGURE 1.1: Schematic of Compliant Journal Bearing (Source- Reddy Amith Hanumappa, (2005), [16])

Figure 1.1 shows the overall look of a compliant journal bearing. As opposed to a conventional journal bearing, it consists of an outer bearing sleeve or an outer housing which contains a round series of bumps over a thin foil strip. A thin smooth top foil sheet is placed

over the bump foil. Now these foils are connected mostly by welding at one of the ends known as the leading edge and are open at the other end called the trailing edge. The uniqueness of a compliant journal bearing over any other conventional bearing is the fact that the bump supports the top foil and act as a spring, hence the bearing is known as compliant. The journal has an interference fit with very negligible clearance, as a result the journal and the foils are in metal to metal contact when the shaft is stationary but as soon as a critical lift-off speed is achieved the journal rotates on a thin gas film due to the hydrodynamic pressure developed. As a result of this hydrodynamic pressure the top foil deforms and forces it away from the shaft towards the bump strip.

The application of forces, which act perpendicular to direction of rotation of shaft, is shown in **figure 1.2.** The hydrodynamic pressure is a function of operating speed and thus influences the deformation of foils. Thus in a nutshell we can say that the film thickness varies with the hydrodynamic pressure as well as the physical, rather elastic properties of the foils. The clearance in radial direction in this type of bearings also represents important criteria which influences the overall performance of the bearing.

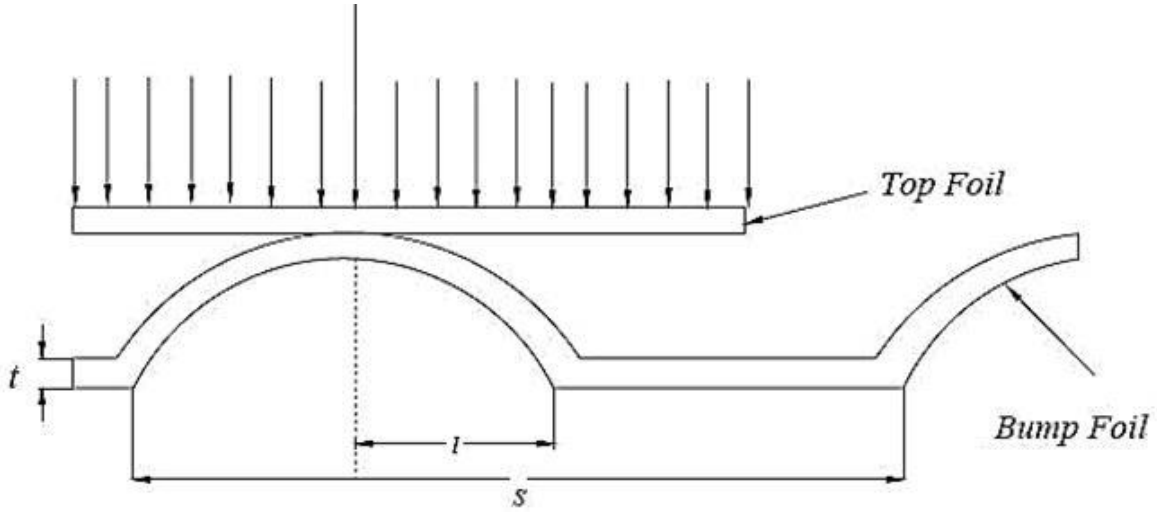

FIGURE 1.2: Schematic of Compliant Journal Bearing showing thickness, length, and pitch (Source- Reddy Amith Hanumappa, (2005), [16])

1.4 ADVANTAGE OF COMPLIANT NATURE OF BEARING

A unique advantage of compliant materials is that they have a certain degree of elastic self-aligning. The elastic deformation compensates for misaligning or other manufacturing errors

of the bearing or sleeve. In contrast metal bearings are very sensitive to any deviation from a perfect roundness of the bearing and journal. For hydrodynamic metal bearings high precision as well as perfect surface finish is essential for successful performance with minimum contact between the surface asperities. In comparison plastic bearings can be manufactured with lower precision due to their compliance characteristic. The advantage of surface compliance is that it relaxes the requirement for high precision which involves high cost.

Moreover the compliant surfaces usually have better wear resistance. Elastic deformation prevents removal of material due to rubbing of rough and hard surfaces. Compliant materials allow the rough asperities to pass through without any wear. In addition it has better wear resistance in the presence of abrasive particles in the lubricant, such as dust, sand etc. Rubber sleeves are often used with slurry lubricant in pumps. Embedding of the abrasive particles in the sleeve is possible by means of elastic deformation.

For all these advantages bearings made up of compliant plastic materials is widely used However their application is limited to light loads and moderates speeds.

CHAPTER - 2

LITERATURE SURVEY

Christopher Dellacorte, Antonio R. Zaldana, Kevin C. Radil [1]

The authors made an exclusive research to find out the load capacity of air foil bearings and thus concluded that adequate design of geometry, smoothness of surface finish; proper lubrication and wear resistance are three important criteria for achieving good load capacity. If any of the three criteria is not met the life of the bearing is shortened. Their research paper showed an approach where the solid lubrication is given by a blend of self-lubricating shaft coatings and other wear resistant and lubricated foil coatings. Due to the use of more than one material with each one of them performing different functions, is designed according to oil lubricated hydrodynamic sleeve bearing technology where different types of coatings and treatments of the surfaces along with the lubricants to achieve the best working performance. The authors of this research work performed the various experiments on journal foil air bearings operating at 1400 rotations per minute. Plasma sprayed composites, polymer, ceramic, inorganic lubricants etc. were some of the coating technologies used for foil bearing lubricants. Their results indicated that through testing of various treatments and use of different lubricants the performance of the bearings is improved. The unique feature of this research is that the combination of several solid lubricants produced better performance of the bearings along with higher life than is achieved by any of the lubricants working alone.

By Stefano Morosi, Ilmar F.Santos [2]

The authors published a paper to lay the theoretical basis for application of active control to gas lubricated journal bearings. The present motivation behind the paper is to demonstrate the degree to which application of active lubrication to gas journal bearings is feasible. The basic principle lies in generation of active forces. This is obtained by regulating the injection of lubricants in radial direction with the help of piezoelectric actuators which are clamped on the back of bearing sleeves. The authors also developed a mathematical model which couples the dynamics of rotor bearing system with the dynamics and mechanics of the actuators through a simple proportional derivative feedback system. They also proved through various numerical examples that this kind of bearing offers several advantages in comparison to conventionally lubricated bearings. The main advantages are the notable reduction in the synchronous

vibration, effective addressal of the half frequency whirling motion and extending of the range of application of gas bearings. It was also prove that this type of bearing improves transient response characteristics, and thus has a better capability of responding to sudden shocks and excitations which the entire system may be subjected to. Due to the addition of active lubrication several new parameters and variables are added to the analysis of the system. The working of the system depends mostly on the proper choice of the control gains, which are particularly different and depends on the goal of the controller. In the future efforts both numerically and experimentally can be aimed for confirming the theoretical findings of this research and thus identify the parameters for tuning the active system at the optimum level.

By Christopher Della Corte, Kevin C. Radil, Robert J. Bruckner & S. Adam Howard [3]

The general lag in familiarization of the design and manufacturing of the foil bearings has led to lack of widespread knowledge and application of gas foil bearings. This research work makes a study on the available literature to show the design; fabrication and testing of the working of both the first and second generation of foil bearings with bump style. This paper could be taken as a standard for beginning new developmental activities for foil bearing technology. The load carrying capacity in terms of coefficient tested at 25degrees was found to be 0.27+/- 0.03 for Generation I and 0.54+/-0.05 for Generation II bearings. The error represents the standard deviation of data and also the results were found to be within the range of expected values of bearings basted upon the historical data available. However this research is not considered for the design, manufacturing of Generation III bearings, though the Generation III bearings have been found to have load carrying capacity coefficient nearly double and triple of Generation II and Generation III bearings respectively.

A unique tooling technique was employed for doing modifications in the bump foil design without actually manufacturing all the ne tooling. All the bearings which were manufactured through this technique were compared with the data already available and were even predicted by modern models which are based on ‘rule of thumb’ law. A very good similarity was found between the experimental values obtained and the data present in literature and the values predicted through the model. The authors found a new thing through this paper that there exists a direct relationship between the complexity of the elasticity of the support system and the working of the bearings. The load carrying capacity, which is one the most

important and most widely uses criteria for comparison of bearings, for bearings which have been modelled simply was the lowest. However for the bearings in which the foundation was modelled according to the system level phenomenon like the misalignment of shafts provided load capacities came out nearly twice than that of the simple bearings. The results of this research should provide for the need and future study of commercially available bearings. Also further study in the direction of advanced geometries of bearings should be done. This is particular to meet the demands of ever growing turbo machinery systems.

By D.Kim, S.Park [4]

The author started by recognizing one of the most critical issues surrounding the reliability of the foil bearings which is a coating wear on the top foil and rotor during the starting and stopping of bearings. Also cooling is sometimes very important under certain applications because the foil bearings can lead to generation of considerable amount of heat depending particularly upon the operating conditions. The space between the top foil and the bearing sleeve is filled with axial flow in most of cases. This thesis introduces a hybrid foil bearing with external pressurized. The advantage of the hybrid nature leads to elimination of coating wear during start/stop of bearings. Also it leads to reduction of the drag torque during start-up. Further a hybrid system does now require any cooling system. The author demonstrated the high potential of this hybrid air foil bearings under hydrostatic mode since its comparison with that of hydrodynamic foil bearings in terms of load capacity was measured at 20000 rpm. Thus it was found that hybrid bearing has a much higher load carrying capacity than hydrodynamic bearing. The author used a simple analytical model to find out the deflection of the top foil under hydrostatic pressurization. Orbit simulations were used to simulate the hybrid air foil bearings and was thus predicted that it has a much higher critical speed and starting speed of instability than its hydrodynamic counterpart. For achieving a realistic top foil deflection system in hybrid operation, sagging effect on the top foil was used through the 1-dimensional beam model, while the orbit simulation model was implemented to predict the imbalance responses which are basically the critical speed and onset speed of unstableness. The simulations show that these properties can have much higher values as compared to the hydrodynamic bearings. As compared to the hydrodynamic bearings, the smaller clearance leads to higher onset speed of instability in hybrid operations. The author also found that higher starting speed of instability could be obtained with the help of increase in stiffness of the spring and correspondingly increase in the air supply pressure. Also a much higher load

carrying capacity was observer with rather less air consumption. This lesser amount of consumption of air proves to be a noticeable advantage of hybrid air foil bearing both in terms of efficiency as well as cooling capacity. The injection of air directly can lead to cooling of both rotor and air film, also the distortion of rotor thermally can be minimised. This factor is really important since the expansion of rotor is one of the bearing failure causes in a variety of applications. Also the starting torque being relatively small implies that the hybrid nature of air foil has the ability to eliminate wear problems, one of the chronic failure modes in several commercial bearings.

By Daejong Kim, Soongook Park [10]

This research paper throws light on the design; construction and testing of the first air foil bearing abbreviated as HAFB. It was compared with its hydrodynamic counterpart. The hybrid case was noticeable with much higher load capacity and much less air consumption. These two factors are particularly advantageous in terms of efficiency and cooling capacity. Also the direct injection of air leads to minimization of thermal distortion of the rotor. Another factor was that the starting torque in hybrid bearings was much lower than the friction torque under steady state operation of hydrodynamic bearings which helps to eliminate the wear problem.

By V.Arora, P.J.M. Van Der Hoogt, R.G.K.M. Aarts, A. De Boer [5]

In the present research work, stiffness and damping are the two main properties of radial air foil bearings which have been identified. In air foil bearings the initial torque required is large, hence in the experimental setup single air foil bearing is employed instead of the usual two foil bearing. The entire set of experiments is performed at 60000 rpm. For identification of stiffness and damping properties the approach used is sub structuring in nature. The developed procedure is found to accomplish the task of identification of the properties. The authors found that one of the major factors which determine the efficiency of a system with air foil bearings is the torque loss. It usually occurs in the air layer between the shaft and the top foils. During operation at high speeds the shearing of air film would cause a torque loss which comes out to be proportional to the speed of rotation. It is actually possible and quite easy to measure the spindle's output torque in different steady running conditions but because of the presence of roller bearings in motor and also the electrical losses in coils contribute in the error in the measured/estimated toque. Hence a torque measurement through mechanical means is devised using the existing experimental setup. Thus the structural properties were identified individually and then were used in developing the finite model of the rotor bearing

support system. The author has also developed a new identification algorithm for the air foil bearing. This algorithm depends on the inverse Eigen sensitivity method. It uses the Eigen data for identifying the other structural characteristics of the bearings. From the results from identification, the author has concluded that during operation at very high speeds, the hardening effects are usually observed. Also it is noticed that the stifnesses calculated from the curve of force vs. deflection are very much comparable with the stiffness identified from the algorithm.

By Howard Samuel A., Dykas Brian [6]

At NASA Glenn Research Centre, during exhaustive testing of air foil journal bearings shaft failure was seen again and again at high ambient temperature and rotational speed at moderate amount of radial load. It is found that the cause of failure is large amount of non-uniform shaft growth which leads to localized viscous heating of the gas film. This eventually leads to rubbing at high speed and finally the destruction of the bearing and the journal. The main result of this research was that it was concluded that centrifugal loading of imbalance correction weights and axial temperature gradients inside the journal (due to the hydrodynamic nature of the foil) were mainly responsible for the non- economic growth of shaft. Since the nature of foil bearings is complex and they operate at extreme conditions it would be inappropriate to directly measure the effect of journal cross-sectional shape distortion at the conditions where actual failure has happened. The author has proposed a failure mechanism which includes two separate effects whose combined effect is solely responsible for shaft failure at extreme operating conditions. Finite element analysis (FEA) is used to represent the observed failure though it is also shown through experiments. The conditions where journal actually fails usually lie outside the typical operating range. The bearings were tested at extremely high ambient temperature with absolutely no cooling air along with a thin walled journal, bearing destruction is possible. Since the drive is much more efficient designs using lightweight foils push the Turbomachine toward thinner lighter shafts and much higher bearing temperatures. Thus with the help of this mechanism and through careful design, failure can be prevented.

By C. DellaCorte, M.J. Valco [7]

The two renowned author introduce a standard ’Rule of Thumb’ to find out the load capacity of air foil journal bearings considered for Turbomachinery applications. The Rule of thumb is based on the data already available in the literature and it relates the load capacity to the

bearing size and speed through a load capacity coefficient – D. The load capacity is a linear function of bearing surface velocity and the projected area. It also depends on the bearing compliant members and the operating conditions, speed and ambient temperature. The earlier bearing designs or popularly known as first generation bearings have comparatively lower load capacity. The second generation compliant support elements are tailored to have much higher load capacity. The limited amount of experimental data available is found to match with the data obtained from linearly approximated Role of Thumb equation. Thus with the help of this equation, the performance that is the load capacity coefficients at different bearing operating conditions can be compared. First generation on bearings have load capacity coefficients of 0.1 to 0.3, second generation has these coefficients from 0.4 to 0.8 while the third generation capacity coefficients are found to be greater than 0.9. The other important bearing parameters which must be considered during assessment of foil bearings for Turbomachinery are the damping and the stiffness. These parameters are required for rotodynamic stability. The stiffness of the bearing is obtained from a combination of the compression of fluid film and the elastic deformation of the foil structure. As compared to the rigid bearings where only limited damping can occur, considerable amount of damping occurs in both the fluid film and in the foil structure of the air foil bearings. The author has found that a bearing with larger load capacity for a given application can be design properly to give way for better stiffness and damping. Thus in the future development of bearing load capacity remains to be an important research goal.

By Hou Yu, Chen Shuangtao, Chen Rugang, Zhang Qiaoyu, Zhao Hongli [12]

In this paper a numerical model was developed which coupled the hydrodynamic pressure of the lubricant film with the deformation of the foil structure. In this model the lubricant was taken as isothermal and isoviscous. And these properties were put to linearize the Reynolds Equation. The top foil was designed in the form of a strip of rectangular thin plate which is supported at a rigid point. The pressure distribution, film thickness and deformation of foil were solved with the help of Finite Element Method. Finally the influence of several parameters like eccentricity ratio, bearing number and number protuberances on performance and life of bearing was studied. The results showed that bearing characteristics are change significantly with increase in the bearing number and eccentricity ratio. Also the hydrodynamic pressure as well as the load capacity as found to be enhanced for this new type of bearing since the top foil with considerable lines of protuberant support tends to warp upwards at the bearing sides due to the bending stresses. This upward warp may lead to

negative film thickness for large eccentricity ratio which represents ill-working of the bearing. Also very few lines of protuberant support can result in the decrease of hydrodynamic pressure, capacity load and frictional torque. On the other hand increasing the lines of protuberant support increases the stiffness of the foil structure and thus reduces its warp.

By Oscar De Santiago, Luis San Andres [14]

Absence of lubricant introduces the possibility of designing the bearings within the flow path of thermal machines. The process gas could also be used as the working fluid for the bearing. Gas foil bearing technologies are found in small compressors for aircraft pressurization, in microturbines and other forms of smaller Turbomachinery. Recent work in the area of foil bearing technology shows that there are calibrated models which help us to accurately predict the performance of the bearings of non-conventional sizes. The main focus of this research work is to make a note of all the parameters of foil bearings which affect the static and dynamic performance and calibrate them for the industrial applications. This is done through a computational model, as a result of which a study on the use of gas foil bearings in a centrifugal compressor for industrial purposes has been done. The first area of investigation suggests that the nonlinear effect of contact between the bumps and the top foil as well as the bumps and carrying sleeve could overtake the response of the bearing thus making the analysis inadequate. The second area of investigation throws light on the fact that this type of bearing has only a limited dynamic stiffness which when combined with the minimum film thickness provides with a load capacity of a few Newton. It is necessary to keep a note on the deflection of bumps behind the top foil at the place where film thickness is minimum. The dynamic load capacity is directly proportional to the linear response of the bearing. One of the areas of future experimental work is related to the use of foil gas bearings in the form of support elements for industrial applications like compressors. The macro mechanism which has been provided determines the load capacity according to the overheating of the top foil. Aging, fretting, pitting, wearing, fatigue etc. of the bump foil are some of the other characteristics which put a limit on the applicability of the foil bearings.

CHAPTER-3

THEORETICAL ANALYSIS OF BEARINGS

The two major needs of hydrodynamic lubrication is

- Requires fluid lubricant: lubricant must be viscous in nature.
- Requires relative motion: movement of one surface over the other must produce a convergent wedge of liquid/gas.

Based upon the needs fluid film lubrication is classified as:

1. **Hydrodynamic or Aerodynamic :**The requirements are

   1.1 Converging edge shape

   1.2 Presence of viscosity

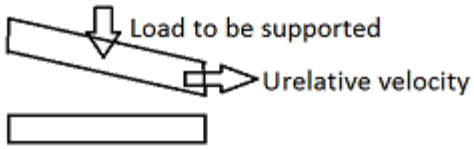

Figure 3.1: Two Converging Plates in Hydrodynamic Lubrication

2. **Squeeze Film:** The requirements are

   2.1 Load or Speed variation

   2.2 Presence of viscosity

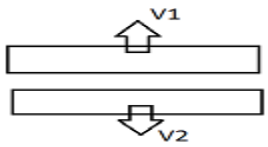

Figure 3.2: Two plates which are non-conversing but velocity of plate changes

3. **Hydrostatic or Aerostatic:** The requirements are

   3.1 External pressure (through a pump etc.)

   3.2 Independent nature to support higher loads

3.1 DERIVATION OF REYNOLDS EQUATION

Considering a finite volume inside the bearing, we apply and equate the forces in different directions:

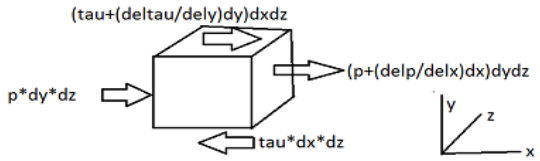

Figure 3.3: Forces applied on a control volume in the bearing

Note that, in the above diagram,

(p+ (delp/delx) dx) dydz is representation for $\left(\text{p} + \frac{\partial p}{\partial x} * dx \right) * dy * dz$

(tau+ (deltau/dely) dy) dx) dz is representation for $\left(\tau + \frac{\partial \tau}{\partial y} * dy \right) * dx * dz$

tau*dx*dz is representation for τ*dy*dz

Balancing the forces in x direction we get, (Assumption 1: inertia terms are negligible)

$$p * dy * dz + \left(\tau + \frac{\partial \tau}{\partial y} * dy \right) * dx * dz = \left(\text{p} + \frac{\partial p}{\partial x} * dx \right) * dy * dz + \tau \text{*dy*dz}$$

$$i.e \ \frac{\partial \tau}{\partial y} = \frac{\partial p}{\partial x} \quad \text{.....3.1}$$

$$For\ la\min ar\ flow\ of\ \ Netonian\ Fluid,\ (Assumption\ 2:\ fluid\ is\ Newtonian)$$

$$\tau = \eta * \frac{\partial u}{\partial y} \quad \text{.....3.2} \quad .$$

From equations 3.1 and 3.2, we get

$$\frac{\partial}{\partial y}(\eta * \frac{\partial u}{\partial y}) = \frac{\partial p}{\partial x} \quad \text{.....3.3}$$

Assumption 3: Negligible pressure gradient in direction of film thickness, y direction

$$Assumption\ 4:\ Coefficient\ of\ \ vis\cos ity,\ \eta\ is\ cons\tan t$$

$$\therefore\ \eta * \frac{\partial}{\partial y}(\frac{\partial u}{\partial y}) = \frac{\partial p}{\partial x} \quad \text{.....3.5}$$

i.e $\frac{\partial p}{\partial x} = \eta * \frac{\partial^2 u}{\partial y^2}$.....3.6

Similarly force balance in z direction we get

$\frac{\partial p}{\partial z} = \eta * \frac{\partial^2 w}{\partial y^2}$.....3.7

Integrating equation 3.6 *we get*

$\eta * \frac{\partial u}{\partial y} = \frac{\partial p}{\partial x} y +$ C1.....3.8

η*u $= \frac{\partial p}{\partial x} \frac{y^2}{2} +$ C1y+ C2.....3.9

At y=0, u=u_2 and

at y=h, u=u_1

Assumption 5: *Assu* min *g no slip at liquid solid boundary,*

i.e. liquid has same boundary as the solid plate

η*$u_2 = C2$.....3.10

η*$u_1 = \frac{\partial p}{\partial x} \frac{h^2}{2} +$ C1h+ η*u_2.....3.11

Solving the above we get

$u = \left(\frac{y^2 - yh}{2 * \eta} \right) \frac{\partial p}{\partial x} + (u_1 - u_2) \frac{y}{h} + u_2$.....3.12

Here $\left(\frac{y^2 - yh}{2 * \eta} \right) \frac{\partial p}{\partial x}$ *is the pressure term*.....3.13

while $(u_1 - u_2) \frac{y}{h} + u_2$ *are the two velocity terms,* u_1 *and* u_2 *being the* max *imum and* min *imum velocity respectively.*

Similarly in z direction we get,

$w = \left(\frac{y^2 - yh}{2 * \eta} \right) \frac{\partial p}{\partial z} + (w_1 - w_2) \frac{y}{h} + w_2$.....3.14

Assumtion 6: *Incompressible fluid*

The equation of continuity or conservation of mass for three dim *ensional incompressible flow is given by,*

$\frac{\partial u}{\partial x} + \frac{\partial v}{\partial y} + \frac{\partial w}{\partial z} = 0$.....3.15

Solving the above we get

$$u = \left(\frac{y^2 - yh}{2*\eta}\right)\frac{\partial p}{\partial x} + (u_1 - u_2)\frac{y}{h} + u_2 \quad \text{.....3.16}$$

Here $\left(\frac{y^2 - yh}{2*\eta}\right)\frac{\partial p}{\partial x}$ *is the pressure term*

while $(u_1 - u_2)\frac{y}{h} + u_2$ *are the two velocity terms,* u_1 *and* u_2 *being the* max *imum and* min *imum velocity respectively.*

Similarly in z direction we get,

Assumption 7: Neflecting the angle of inclination for coordinate system

Integrating the continuity equation in y direction from $y = 0$ *to* $y = h$*,*

U sin *g Leibnitz Rule,*

$$\int_a^b \frac{\partial u(y,x)}{\partial x}dy = \frac{\partial}{\partial x}\left(\int_a^b u dy\right) - u(b,x)\frac{db}{dx} + u(a,x)\frac{da}{dx} \quad \text{.....3.17}$$

In our case the Leibnitz equation becomes,

$$\int_0^h \frac{\partial u(x,y)}{\partial x}dy = \frac{\partial}{\partial x}\left(\int_0^h u(x,y)dy\right) - u(x,h)\frac{dh}{dx} + u(x,0)\frac{d0}{dx} \quad \text{.....3.18}$$

$$u(x,0)\frac{d0}{dx} = 0 \quad \text{.....3.19}$$

$$\therefore \int_0^h \frac{\partial u}{\partial x}dy = \frac{\partial}{\partial x}\left(\int_0^h u dy\right) - u_1\frac{\partial h}{\partial x} \quad \text{.....3.20}$$

$$\int_0^h u dy = \left[\left[\frac{1}{2\eta}\left(\frac{y^3}{3} - \frac{y^2 h}{2}\right)\right]\frac{\partial p}{\partial x} + \frac{u_1 - u_2}{h} * \frac{y^2}{2} + u_2 y\right]_0^h \quad \text{.....3.21}$$

$$\Rightarrow -\frac{h^3}{12\eta}\frac{\partial p}{\partial x} + \frac{h}{2}(u_1 + u_2) \quad \text{.....3.22}$$

$$\therefore \int_0^h \frac{\partial u}{\partial x}dy = \frac{\partial}{\partial x}\left(-\frac{h^3}{12\eta}\frac{\partial p}{\partial x} + \frac{h}{2}(u_1 + u_2) - u_1\frac{\partial h}{\partial x}\right) \quad \text{.....3.23}$$

$$\Rightarrow \frac{\partial}{\partial x}\left(-\frac{h^3}{12\eta}\frac{\partial p}{\partial x} + \frac{h}{2}(u_1 + u_2) - u_1 h\right) \quad \text{.....3.24}$$

$$\Rightarrow -\frac{\partial}{\partial x}\left(\frac{h^3}{12\eta}\frac{\partial p}{\partial x}\right) - \frac{1}{2}\frac{\partial}{\partial x}(u_1 - u_2)h\Big) \quad \text{.....3.25}$$

Similarly in z direction:

$$\int_0^h \frac{\partial w}{\partial z} dy = -\frac{\partial}{\partial z}\left(\frac{h^3}{12\eta} * \frac{\partial p}{\partial z}\right) - \frac{1}{2}\frac{\partial}{\partial z}\left((w_1 - w_2)h\right) \quad \text{.....3.26}$$

Hence on int*egrating the continuity equation* 3.16:

$$\int_0^h \frac{\partial u}{\partial x} dy + \int_0^h \frac{\partial v}{\partial y} dy + \int_0^h \frac{\partial w}{\partial z} dy = 0 \quad \text{.....3.27}$$

$$\Rightarrow -\frac{\partial}{\partial x}\left(\frac{h^3}{12\eta}\frac{\partial p}{\partial x}\right) - \frac{1}{2}\frac{\partial}{\partial x}\left((u_1 - u_2)h\right) + (v_1 - v_2) - \frac{\partial}{\partial z}\left(\frac{h^3}{12\eta}\frac{\partial p}{\partial z}\right) - \frac{1}{2}\frac{\partial}{\partial z}\left((w_1 - w_2)h\right) = 0 \quad \text{.....3.28}$$

$$\Rightarrow \frac{\partial}{\partial x}\left(\frac{h^3}{12\eta}\frac{\partial p}{\partial x}\right) + \frac{\partial}{\partial z}\left(\frac{h^3}{12\eta}\frac{\partial p}{\partial z}\right) = \frac{1}{2}\frac{\partial}{\partial x}\left((u_2 - u_1)h\right) + (v_1 - v_2) + \frac{1}{2}\frac{\partial}{\partial z}\left((w_2 - w_1)h\right) \quad \text{.....3.29}$$

In the above equation :

Left Hand Side Terms are the PRESSURE TERMS

Right Hand Side Terms are the SOURCE TERMS

$\frac{\partial h}{\partial x}$ and $\frac{\partial h}{\partial z}$ *are the WEDGE TERMS*

$\frac{\partial u}{\partial x}$ and $\frac{\partial w}{\partial z}$ *are the STRETCHING ACTION TERMS*

$(v_1 - v_2)$ *is the SQUEEZE ACTION terms*

Also the squeeze action term can be written as:

$$(v_1 - v_2) = \frac{\partial h}{\partial t} \quad \text{.....3.30}$$

Thus the Re*ynolds equation comes out to be*:

$$\frac{\partial}{\partial x}\left(\frac{h^3}{12\eta}\frac{\partial p}{\partial x}\right) + \frac{\partial}{\partial z}\left(\frac{h^3}{12\eta}\frac{\partial p}{\partial z}\right) = \frac{1}{2}\frac{\partial}{\partial x}\left((u_2 - u_1)h\right) + \frac{\partial h}{\partial t} + \frac{1}{2}\frac{\partial}{\partial z}\left((w_2 - w_1)h\right) \quad \text{.....3.31}$$

*However for perfor*min*g more in a real world situation, our research work consists of compressible* lub*ricant that is density is not a cons*tan*t, thus assumption 7 is cancelled*.

Hence the final Re*ynolds equation under compressible condition comes out to be,*

$$\frac{\partial}{\partial x}\left(\frac{\rho h^3}{12\eta}\frac{\partial p}{\partial x}\right) + \frac{\partial}{\partial z}\left(\frac{\rho h^3}{12\eta}\frac{\partial p}{\partial z}\right) = \frac{1}{2}\frac{\partial}{\partial x}(\rho(u_2 - u_1)h) + \frac{\partial h}{\partial t} + \frac{1}{2}\frac{\partial}{\partial z}(\rho(w_2 - w_1)h) \quad \text{.....3.32}$$

Assumption 8: Re*lative* tan*gential velocity only in x direction and not in z direction*

$$\Rightarrow \frac{1}{2}\frac{\partial}{\partial z}(\rho(w_2 - w_1)h) = 0 \quad \text{.....3.33}$$

Assumption 9: *Both surfaces are rigid or in other words no stretching action*

$$\Rightarrow \frac{1}{2}\frac{\partial}{\partial x}(\rho(u_2-u_1)h) = (u_2-u_1)*\frac{1}{2}*\frac{\partial(\rho h)}{\partial x} \quad \text{.....3.34}$$

Assumtion 10: *The top surface is stationary* or $u_1 = 0$

$\Rightarrow u_2 = u$

Assumption 11: *Steady state operation of the bearing*

$$\frac{\partial h}{\partial t} = 0 \quad \text{.....3.35}$$

Thus the final Re *ynolds equation taking* int *o account all the assumptions is*:

$$\frac{\partial}{\partial x}\left(\frac{\rho h^3}{12\eta}\frac{\partial p}{\partial x}\right) + \frac{\partial}{\partial z}\left(\frac{\rho h^3}{12\eta}\frac{\partial p}{\partial z}\right) = \frac{u}{2}\frac{\partial(\rho h)}{\partial x} \quad \text{.....3.36}$$

3.2 REYNOLDS EQUATION IN POLAR COORDINATES

U sin *g polar coordinates the two impor* tan *t transformation equations are*:

1. $x = R\theta \Rightarrow \partial x = R\partial\theta$ 3.37
2. $u = R\omega$ 3.38

Thus we get

$$\frac{1}{R}\frac{\partial}{\partial\theta}\left(\frac{\rho h^3}{12\eta}*\frac{1}{R}\frac{\partial p}{\partial\theta}\right) + \frac{\partial}{\partial z}\left(\frac{\rho h^3}{12\eta}\frac{\partial p}{\partial z}\right) = \frac{R\omega}{2}\frac{\partial(\rho h)}{R\partial\theta} \quad \text{.....3.39}$$

Considering ideal gas equation i.e. $\rho = \frac{p}{R_g T}$

$$\frac{1}{R}\frac{\partial}{\partial\theta}\left(\frac{ph^3}{12\eta R_g T}*\frac{1}{R}\frac{\partial p}{\partial\theta}\right) + \frac{\partial}{\partial z}\left(\frac{ph^3}{12\eta R_g T}\frac{\partial p}{\partial z}\right) = \frac{\omega}{2}\frac{\partial}{\partial\theta}\left(\frac{ph}{R_g T}\right) \quad \text{.....3.40}$$

Multiplying by $R^2 R_g$

$$\frac{\partial}{\partial\theta}\left(\frac{ph^3}{12\eta T}\frac{\partial p}{\partial\theta}\right) + R^2\frac{\partial}{\partial z}\left(\frac{ph^3}{12\eta T}\frac{\partial p}{\partial z}\right) = \frac{\omega R^2}{2}\frac{\partial}{\partial\theta}\left(\frac{ph}{T}\right) \quad \text{.....3.41}$$

3.3 NON-DIMENSIONALIZATION

With the help of normaliztion or non dim *ensionalization*

$$\bar{z}=\frac{z}{\frac{L}{2}};\bar{p}=\frac{p}{p_a};\bar{h}=\frac{h}{C};\bar{\eta}=\frac{\eta}{\eta_0};\bar{T}=\frac{T}{T_0} \quad \text{.....3.42}$$

$$\Rightarrow \frac{\partial}{\partial\theta}\left(\frac{\bar{p}p_a\bar{h}C^3}{12\bar{\eta}\eta_0\bar{T}T_0}\left(\frac{\partial}{\partial\theta}(\bar{p}p_a)\right)\right)+R^2\frac{\partial}{\frac{L}{2}\partial\bar{z}}\left(\frac{\bar{p}p_a\bar{h}^3C^3}{12\bar{\eta}\eta_0\bar{T}T_0}\left(\frac{\partial}{\frac{L}{2}\partial\bar{z}}(\bar{p}p_a)\right)\right)=\frac{\omega R^2}{2}\frac{\partial}{\partial\theta}\left(\frac{\bar{p}p_a\bar{h}C}{\bar{T}T_0}\right) \quad \text{.....3.43}$$

Assumtion: *U* sin *g Isothermal and Isoviscous* lub *ricant*

$$\Rightarrow \bar{\eta}=1 \text{ and } \bar{T}=1 \quad \text{.....3.44}$$

$$\Rightarrow \frac{\partial}{\partial\theta}\left(\bar{p}\bar{h}^3\left(\frac{\partial\bar{p}}{\partial\theta}\right)\right)+\frac{{p_a}^2C^3}{12\eta_0T_0}*\frac{R^2}{\left(\frac{L}{2}\right)^2}\frac{\partial}{\partial\bar{z}}\left(\bar{p}\bar{h}^3\frac{\partial\bar{p}}{\partial\bar{z}}\right)*\frac{12\eta_0T_0}{{p_a}^2C^3}=\frac{12\eta_0T_0}{{p_a}^2C^3}*\frac{\omega R^2}{2}*\frac{p_aC}{T_0}\frac{\partial(\bar{p}\bar{h})}{\partial\theta} \quad \text{.....3.45}$$

Taking Compressibility or Bearing Number as:

$$\Lambda=\frac{6\omega\eta_0}{p_a}\left(\frac{R}{C}\right)^2 \quad \text{.....3.46}$$

we get the STANDARDCOMPRESSIBLE REYNOLDS EQUATION IN 2 *DIMENSIONS as*:

$$\frac{\partial}{\partial\theta}\left(\bar{p}\bar{h}^3\left(\frac{\partial\bar{p}}{\partial\theta}\right)\right)+\left(\frac{2R}{L}\right)^2\frac{\partial}{\partial\bar{z}}\left(\bar{p}\bar{h}^3\frac{\partial\bar{p}}{\partial\bar{z}}\right)=\Lambda\frac{\partial(\bar{p}\bar{h})}{\partial\theta} \quad \text{.....3.47}$$

3.4 EXPANSION OF REYNOLDS EQUATION

Expanding the Re *ynolds Equation term by term we get*,

$$\text{L.H.S.}=\bar{p}\bar{h}^3\frac{\partial^2\bar{p}}{\partial\theta^2}+\bar{p}*3\bar{h}^2*\frac{\partial\bar{p}}{\partial\theta}*\frac{\partial\bar{h}}{\partial\theta}+\bar{h}^3\left(\frac{\partial\bar{p}}{\partial\theta}\right)^2+\left(\frac{2R}{L}\right)^2\left[\bar{p}\bar{h}^3\frac{\partial^2\bar{p}}{\partial\bar{z}^2}+\bar{p}*3\bar{h}^2*\frac{\partial\bar{p}}{\partial\bar{z}}*\frac{\partial\bar{h}}{\partial\bar{z}}+\bar{h}^3\left(\frac{\partial\bar{p}}{\partial\bar{z}}\right)^2\right].$$

.....3.48

$$\text{R.H.S.}=\Lambda\left[\bar{p}\frac{\partial\bar{h}}{\partial\theta}+\bar{h}\frac{\partial\bar{p}}{\partial\theta}\right] \quad \text{.....3.49}$$

Assu min *g h to be a fuction of only* θ *and not z*

$$\Rightarrow \frac{\partial\bar{h}}{\partial\bar{z}}=0 \quad \text{.....3.50}$$

Expanded Re *ynolds Equation comes out to be*:

$$\frac{\partial^2\bar{p}}{\partial\theta^2}+\left(\frac{2R}{L}\right)^2\frac{\partial^2\bar{p}}{\partial\bar{z}^2}=-\frac{3}{\bar{h}}\left[\frac{\partial\bar{p}}{\partial\theta}*\frac{\partial\bar{h}}{\partial\theta}\right]-\frac{1}{\bar{p}}\left[\left(\frac{\partial\bar{p}}{\partial\theta}\right)^2+\left(\frac{2R}{L}\right)^2\left(\frac{\partial\bar{p}}{\partial\bar{z}}\right)^2\right]+\frac{\Lambda}{\bar{h}^3}\frac{\partial\bar{h}}{\partial\theta}+\frac{\Lambda}{\bar{p}\bar{h}^2}\frac{\partial\bar{p}}{\partial\theta} \quad \text{.....3.51}$$

3.5 FINAL ASSUMPTIONS

- *Negligible inertia terms*
- *Negligible change in film thickness in z direction i.e. h varies with only θ*
- *Newtonian Fluid*
- *Constant coefficient of viscosity (η=constant)*
- *No slip of liquid solid Boundary*
- *Neglecting angle of inclination for the coordinate system*
- *Compressible but ideal gas flow*
- *Relative tangential velocity in x – direction*
- *Both the surfaces are rigid, i.e. no stretching action*
- *Top surface is stationary*
- *Film Thickness, h is a function of only pressure 'p', θ but not z*
- *Steady state operation of bearing or in other words film thickness does not change with time.*

CHAPTER-4

NUMERICAL METHODS

Our next target is to solve the Reynolds Equation:

$$\frac{\partial^2 \bar{p}}{\partial \theta^2} + \left(\frac{2R}{L}\right)^2 \frac{\partial^2 \bar{p}}{\partial \bar{z}^2} = -\frac{3}{\bar{h}}\left[\frac{\partial \bar{p}}{\partial \theta} * \frac{\partial \bar{h}}{\partial \theta}\right] - \frac{1}{\bar{p}}\left[\left(\frac{\partial \bar{p}}{\partial \theta}\right)^2 + \left(\frac{2R}{L}\right)^2 \left(\frac{\partial \bar{p}}{\partial \bar{z}}\right)^2\right] + \frac{\Lambda}{\bar{h}^3}\frac{\partial \bar{h}}{\partial \theta} + \frac{\Lambda}{\bar{p}\bar{h}^2}\frac{\partial \bar{p}}{\partial \theta} \quad \text{.....4.1}$$

Thus we can see that the above Reynolds Equation is:

- 2^{nd} order.
- Non Linear.
- Partial Differential Equation.

4.1 APPROACH TO THE SOLUTION

Hence the Reynolds Equation can be solved only by Numerical Methods. In our research work we have used Finite Difference Method for solving the Reynolds Method. The fundamental difference between Finite Difference Method and Finite Element Method is that in finite element method we tend to compare the forces, stresses and strains developed in the system with the help of equations writing them in matrix form while in Finite Difference Method we change the derivatives or gradients by simple difference formula. Basically these are just the two alternate or optional methods for discretization process. In this method the entire bearing space is divided into an M*N grid system. The pressure values at every node is initialised with certain value, subsequently on every iteration the pressure values are updated. For finding the pressure at any node, pressure values at all the surrounding nodes must be known from the previous iteration. Thus a pressure v/s θ v/s z plot is obtained. From the pressure values the load carrying capacity is obtained.

4.2 MATHEMATICAL CONVERSION

The Reynolds equation is converted into the finite difference form using certain Finite Difference Approximations:

$$\frac{\partial^2 \bar{p}}{\partial \theta^2} = \frac{\bar{p}_{i+1,j} - 2\bar{p}_{i,j} + \bar{p}_{i-1,j}}{\Delta \theta^2} \quad \text{.....4.2}$$

$$\frac{\partial^2 \bar{p}}{\partial \bar{z}^2} = \frac{\bar{p}_{i,j+1} - 2\bar{p}_{i,j} + \bar{p}_{i,j-1}}{\Delta \bar{z}^2} \quad \text{.....4.3}$$

$$\frac{\partial \bar{p}}{\partial \theta} = \frac{\bar{p}_{i+1,j} - \bar{p}_{i-1,j}}{2\Delta\theta} \quad \text{.....4.4}$$

$$\frac{\partial \bar{h}}{\partial \theta} = \frac{\bar{h}_{i+1,j} - \bar{h}_{i-1,j}}{2\Delta\theta} \quad \text{.....4.5}$$

$$\frac{\partial \bar{p}}{\partial \bar{z}} = \frac{\bar{p}_{i,j+1} - \bar{p}_{i,j-1}}{2\Delta\bar{z}} \quad \text{.....4.6}$$

$$\frac{\partial \bar{h}}{\partial \bar{z}} = \frac{\bar{h}_{i,j+1} - \bar{h}_{i,j-1}}{2\Delta\bar{z}} \quad \text{.....4.7}$$

Thus we need to convert the Re*ynolds Equation* int*o the finite difference form*

$$\Rightarrow \frac{\partial^2 \bar{p}}{\partial \theta^2} + (\frac{2R}{L})^2 \frac{\partial^2 \bar{p}}{\partial \bar{z}^2} = -\frac{3}{\bar{h}}\left[\frac{\partial \bar{p}}{\partial \theta} * \frac{\partial \bar{h}}{\partial \theta}\right] - \frac{1}{\bar{p}}\left[(\frac{\partial \bar{p}}{\partial \theta})^2 + (\frac{2R}{L})^2 (\frac{\partial \bar{p}}{\partial \bar{z}})^2\right] + \frac{\Lambda}{\bar{h}^3}\frac{\partial \bar{h}}{\partial \theta} + \frac{\Lambda}{\bar{p}\bar{h}^2}\frac{\partial \bar{p}}{\partial \theta} \quad \text{.....4.8}$$

$$\text{L.H.S.} = \frac{\bar{p}_{i+1,j} - 2\bar{p}_{i,j} + \bar{p}_{i-1,j}}{\Delta\theta^2} + (\frac{2R}{L})^2 \left[\frac{\bar{p}_{i,j+1} - 2\bar{p}_{i,j} + \bar{p}_{i,j-1}}{\Delta\bar{z}^2}\right] \quad \text{.....4.9}$$

$$\text{R.H.S.} = -\frac{1}{\bar{p}_{i,j}}\left[(\frac{\bar{p}_{i+1,j} - \bar{p}_{i-1,j}}{2\Delta\theta})^2 + (\frac{2R}{L})^2 (\frac{\bar{p}_{i,j+1} - \bar{p}_{i,j-1}}{2\Delta\bar{z}})^2\right] - \frac{3}{\bar{h}_{i,j}}\left[\frac{\bar{h}_{i+1,j} - \bar{h}_{i-1,j}}{2\Delta\theta} * \frac{\bar{p}_{i+1,j} - \bar{p}_{i-1,j}}{2\Delta\theta}\right]$$
$$+ \frac{\Lambda}{\bar{h}_{i,j}^3}\frac{\bar{h}_{i+1,j} - \bar{h}_{i-1,j}}{2\Delta\theta} + \frac{\Lambda}{\bar{p}_{i,j}\bar{h}_{i,j}^2}\frac{\bar{p}_{i+1,j} - \bar{p}_{i-1,j}}{2\Delta\theta} \quad \text{.....4.10}$$

$$\frac{\bar{p}_{i+1,j} - 2\bar{p}_{i,j} + \bar{p}_{i-1,j}}{\Delta\theta^2} + (\frac{2R}{L})^2 \left[\frac{\bar{p}_{i,j+1} - 2\bar{p}_{i,j} + \bar{p}_{i,j-1}}{\Delta\bar{z}^2}\right] = -\frac{1}{\bar{p}_{i,j}}\left[(\frac{\bar{p}_{i+1,j} - \bar{p}_{i-1,j}}{2\Delta\theta})^2 + (\frac{2R}{L})^2 (\frac{\bar{p}_{i,j+1} - \bar{p}_{i,j-1}}{2\Delta\bar{z}})^2\right]$$
$$- \frac{3}{\bar{h}_{i,j}}\left[\frac{\bar{h}_{i+1,j} - \bar{h}_{i-1,j}}{2\Delta\theta} * \frac{\bar{p}_{i+1,j} - \bar{p}_{i-1,j}}{2\Delta\theta}\right]$$
$$+ \frac{\Lambda}{\bar{h}_{i,j}^3}\frac{\bar{h}_{i+1,j} - \bar{h}_{i-1,j}}{2\Delta\theta} + \frac{\Lambda}{\bar{p}_{i,j}\bar{h}_{i,j}^2}\frac{\bar{p}_{i+1,j} - \bar{p}_{i-1,j}}{2\Delta\theta} \quad \text{.....4.11}$$

$$\bar{p}_{i,j}^2\left[\frac{2}{(\Delta\theta)^2} + (\frac{2R}{L})^2 * \frac{2}{\Delta\bar{z}^2}\right] + \bar{p}_{i,j}\left[\begin{array}{l} -\frac{\bar{p}_{i+1,j} + \bar{p}_{i-1,j}}{\Delta\theta^2} - (\frac{2R}{L})^2 \frac{\bar{p}_{i,j+1} + \bar{p}_{i,j-1}}{\Delta\bar{z}^2} - \frac{3}{\bar{h}_{i,j}} * \frac{\bar{h}_{i+1,j} - \bar{h}_{i-1,j}}{2\Delta\theta} * \\ \frac{\bar{p}_{i+1,j} - \bar{p}_{i-1,j}}{2\Delta\theta} + \frac{\Lambda}{\bar{h}_{i,j}^3}\frac{\bar{h}_{i+1,j} - \bar{h}_{i-1,j}}{2\Delta\theta} \end{array}\right]$$
$$-\left[(\frac{\bar{p}_{i+1,j} - \bar{p}_{i-1,j}}{2\Delta\theta})^2 + (\frac{2R}{L})^2 (\frac{\bar{p}_{i,j+1} - \bar{p}_{i,j-1}}{2\Delta\bar{z}})^2\right] + \frac{\Lambda}{\bar{h}_{i,j}^2}\frac{\bar{p}_{i+1,j} - \bar{p}_{i-1,j}}{2\Delta\theta} = 0 \quad \text{.....4.12}$$

The above equation can be converted int*o the quadratic form such that,*

$$A\bar{p}_{i,j}^2 + B\bar{p}_{i,j} + C = 0 \quad \text{.....4.13}$$

where $A=\left[\frac{2}{(\Delta\theta)^2}+(\frac{2R}{L})^2*\frac{2}{\Delta\bar{z}^2}\right]$ 4.14

$B=\left[-\frac{\bar{p}_{i+1,j}+\bar{p}_{i-1,j}}{\Delta\theta^2}-(\frac{2R}{L})^2\frac{\bar{p}_{i,j+1}+\bar{p}_{i,j-1}}{\Delta\bar{z}^2}-\frac{3}{\bar{h}_{i,j}}*\frac{\bar{h}_{i+1,j}-\bar{h}_{i-1,j}}{2\Delta\theta}*\frac{\bar{p}_{i+1,j}-\bar{p}_{i-1,j}}{2\Delta\theta}+\frac{\Lambda}{\bar{h}_{i,j}^{\,3}}\frac{\bar{h}_{i+1,j}-\bar{h}_{i-1,j}}{2\Delta\theta}\right]$ 4.15

and $C=-\left[(\frac{\bar{p}_{i+1,j}-\bar{p}_{i-1,j}}{2\Delta\theta})^2+(\frac{2R}{L})^2(\frac{\bar{p}_{i,j+1}-\bar{p}_{i,j-1}}{2\Delta\bar{z}})^2\right]+\frac{\Lambda}{\bar{h}_{i,j}^{\,2}}\frac{\bar{p}_{i+1,j}-\bar{p}_{i-1,j}}{2\Delta\theta}$ 4.16

The process of iterations will be repeated till the specified accuracy is attained by a convergence criterion as:

$$\frac{\left[\sum_{i=1}^{M}\sum_{j=1}^{N}\bar{p}_{i,j}\right]_{k^{th}\text{ iteration}}-\left[\sum_{i=1}^{M}\sum_{j=1}^{N}\bar{p}_{i,j}\right]_{k-1^{th}\text{ iteration}}}{\left[\sum_{i=1}^{M}\sum_{j=1}^{N}\bar{p}_{i,j}\right]_{k^{th}\text{ iteration}}}\le\varepsilon$$

where ε can be used according to the desired level of accuracy such as 0.01, 0.001 *or* 0.0001 *etc.*

4.3 RELATIONS FOR FILM THICKNESS

Now the film thickness is unknown to us. Normally the film thickness is given by the relation:

$h = C + e_f*\cos\theta$

But, since our foil bearing is of compliant nature, the film thickness is also dependent upon the pressure

$h = C + e_f*\cos\theta + \alpha\,(p-1)$

Or

$h_{i,j}=C + e_f*\cos\theta_{i,j} + \alpha(p_{i,j}-1)$

Again normalizing the above relation we get,

$\bar{h} = 1 + \varepsilon_f*\cos\theta + \alpha(\bar{p}-1)$

where $\bar{h}=\frac{h}{C}$, $\varepsilon_f=\frac{e_f}{C}$ and $\bar{p}=\frac{p}{p_a}$

Also α is known as the Compliance Number of the Bearing and is given by the following relation

$\alpha=\frac{2*p_a*s}{C*E}*\left(\frac{l}{t}\right)^3*(1-\upsilon^2)$

4.4 FLOWCHART

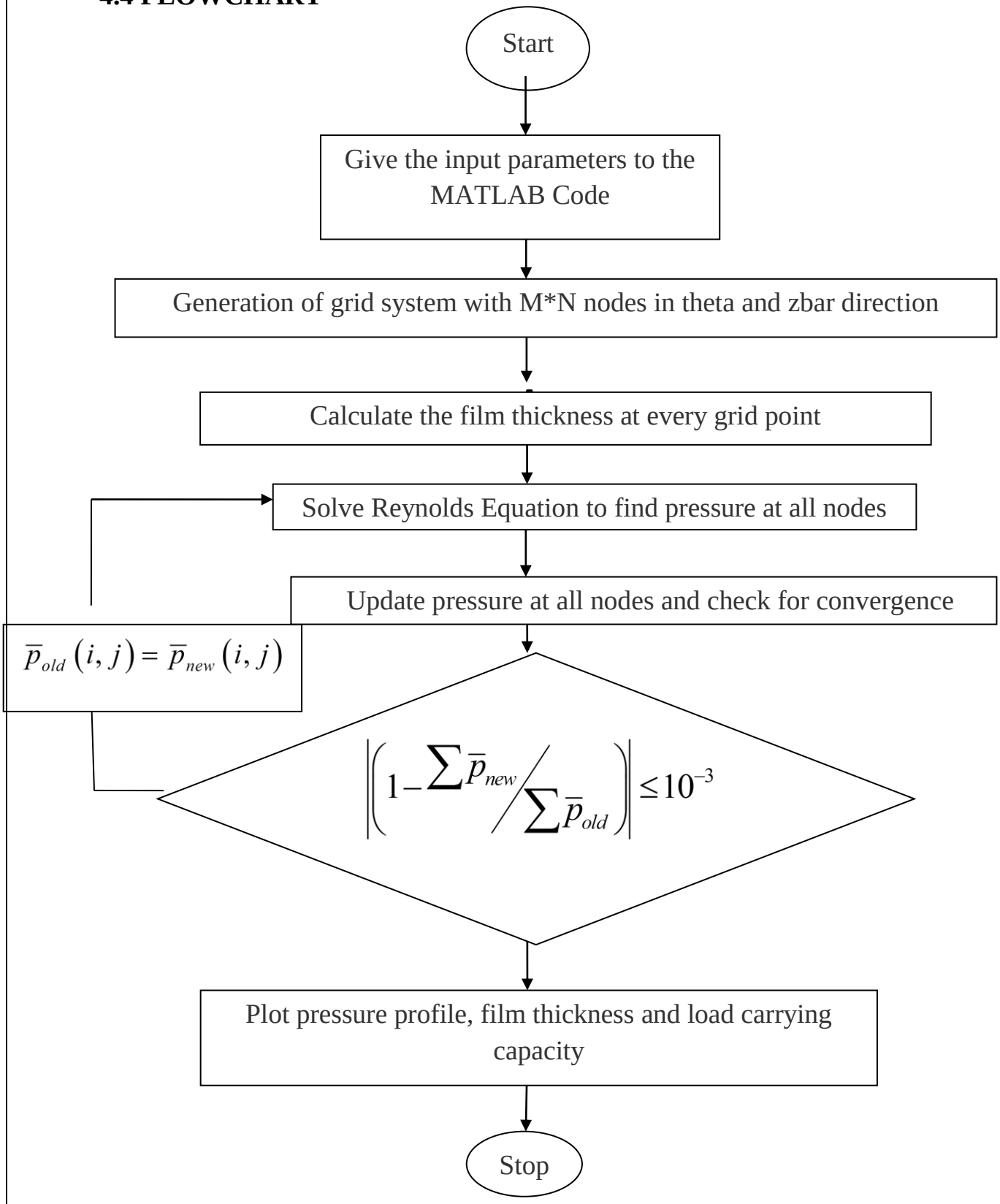

Chapter 5

RESULTS AND DISCUSSIONS

For comparison purposes the MATLAB code was prepared and by giving the various inputs, the results of two different commercially used materials was obtained in terms of

- Pressure profile.
- Load carrying capacity.
- Film Thickness.

Sl. No.	Input Property	Value	Unit
1.	Radial Clearance (C)	0.03	mm
2.	Radius of Shaft (R)	25	mm
3.	Length of bearing (Le)	50	mm
4.	Eccentricity (e)	0.02	mm
5.	Bump pitch (s)	3.17	mm
6.	Atmospheric Pressure (pat)	0.1	N/mm2
7.	Half Bump length (l)	1.125	mm
8.	Thickness of bump foil (t)	0.1	mm
9.	Poisson's ratio (υ)	0.29	-
10.	Viscosity of lubricant(η)	17.8*10-12	N-s/mm2
11.	Angular speed of Rotation (ω)	30000	rpm
12.	Eccentricity ratio eps = e/C	0.67	-
13.	Modulus of Elasticity of bump foil (Et)	212000	N/mm2
14.	No. of grid points in theta direction (M)	50	-
15.	No. of grid points in zbar direction (N)	50	-
16.	No. of iterations	1000	-

Table 5.1: Input properties with Inconel X-750 as bump foil material

5.1 ANALYSIS OF MATERIAL OF BUMP FOIL: INCONEL X-750

The first material to be selected was Inconel X-750 since it is one of the bump foil materials used in manufacturing the bump foils of bearings chiefly employed in high temperature applications. Inconel X-750 basically is a Nickel-Chromium alloy made of additions of Aluminium and Titanium, having creep-rupture strength at high temperatures to about 700°C. Some of the areas of application of Inconel X-750 are:

- Nuclear reactors
- Gas Turbine
- Rocket Engines

With the help of the properties as mentioned in table5.1, the MATLAB Code is solved for certain fixed number of iterations. Inconel X-750 has Poisson's Ratio of 0.29 and Modulus of Elasticity of 212GPa, these being the two most important mechanical properties of the bump foil material.

5.1.1 PRESSURE PROFILE

The three dimensional pressure profile under the given input parameters for bump foil made of Inconel X-750 comes out to be as shown in the next page. As we can see that theta varies from 0 to 2π i.e. from 0 to 6.28. Similarly the zbar axis varies from 0 to 1. The pressure profile is represented in the form of non-dimensional pressure (p/p_a).

Upto a little distance from the leading edge, and considerable more distance from the trailing edge the pressure profile is atmospheric in nature. This is due to the detachment of the foils. Thus the pressure is generated at a certain angle, keeps on increasing to maximum value and then settles down to atmospheric value.

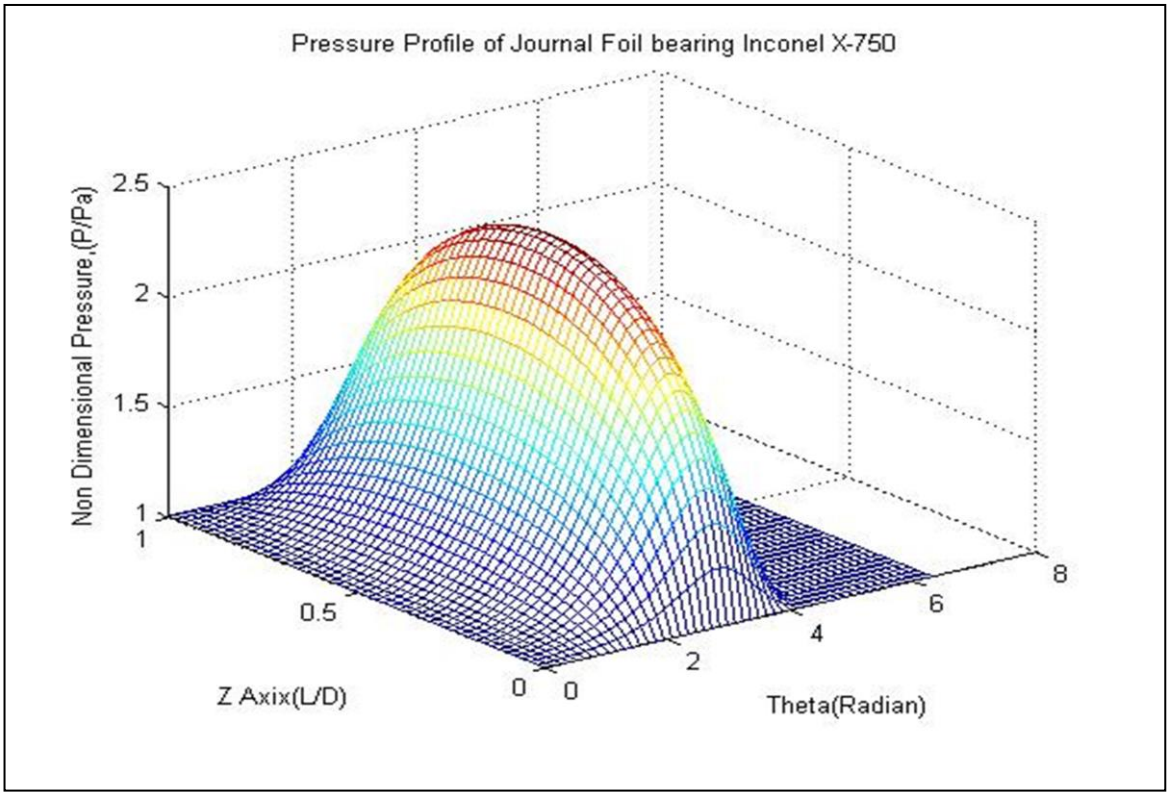

Figure 5.01: Pressure profile of journal foil bearing for Inconel X-750

5.1.2 Non Dimensional Film Thickness

The 3D plot of non-dimensional film thickness under the given input parameters for bump foil made of Inconel X-750 comes out to be as shown in the next page. The film thickness varies only in theta direction and not in z direction. During initial rotation of shaft i.e. at initial value of shaft the film thickness is higher but then the air film becomes lesser and lesser in thickness. Again after a certain degree of rotation, the film thickness again starts increasing.

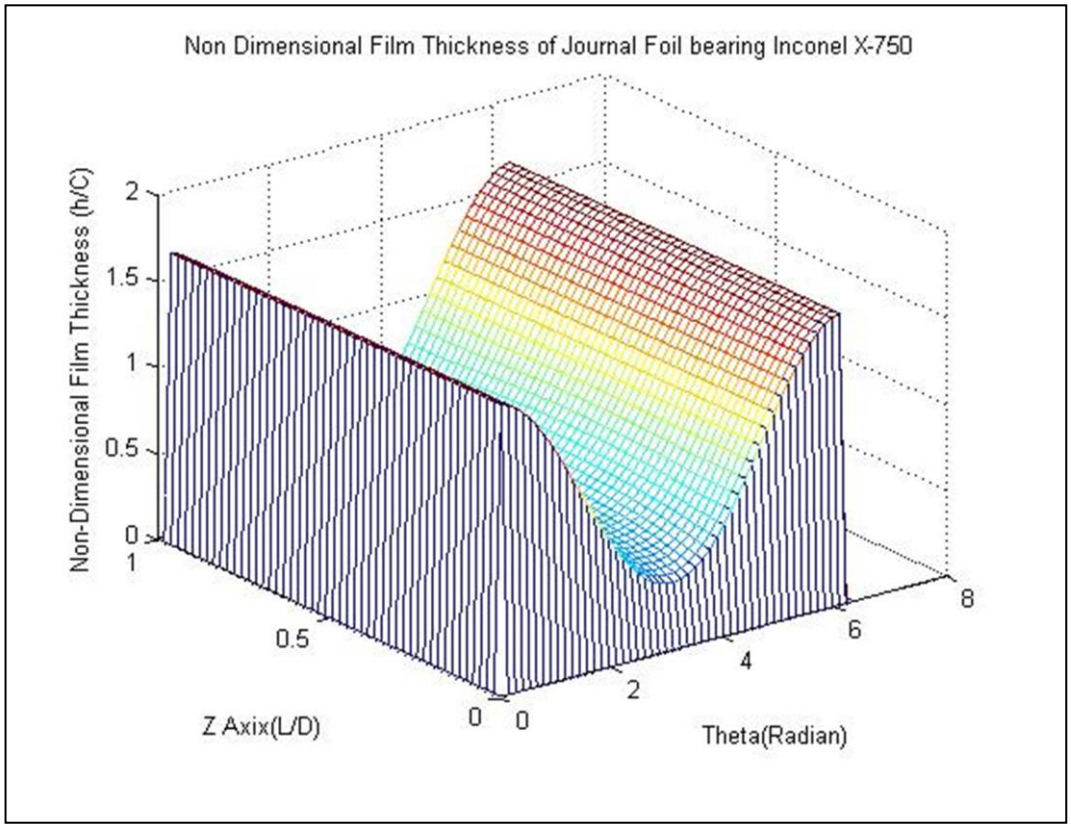

Figure 5.02: Non-Dimensional Film Thickness for Inconel X-750

5.1.3 Comparison of Foil Bearing with Rigid Bearing

The film thickness in case foil bearing differs with that of rigid bearing. Due to the difference in the film thickness the pressure profile differs. We can see that lower film thickness can be obtained in case of foil bearing. The film thickness of foil bearing is close to the rigid bearing and higher than expected total roughness of two surfaces.

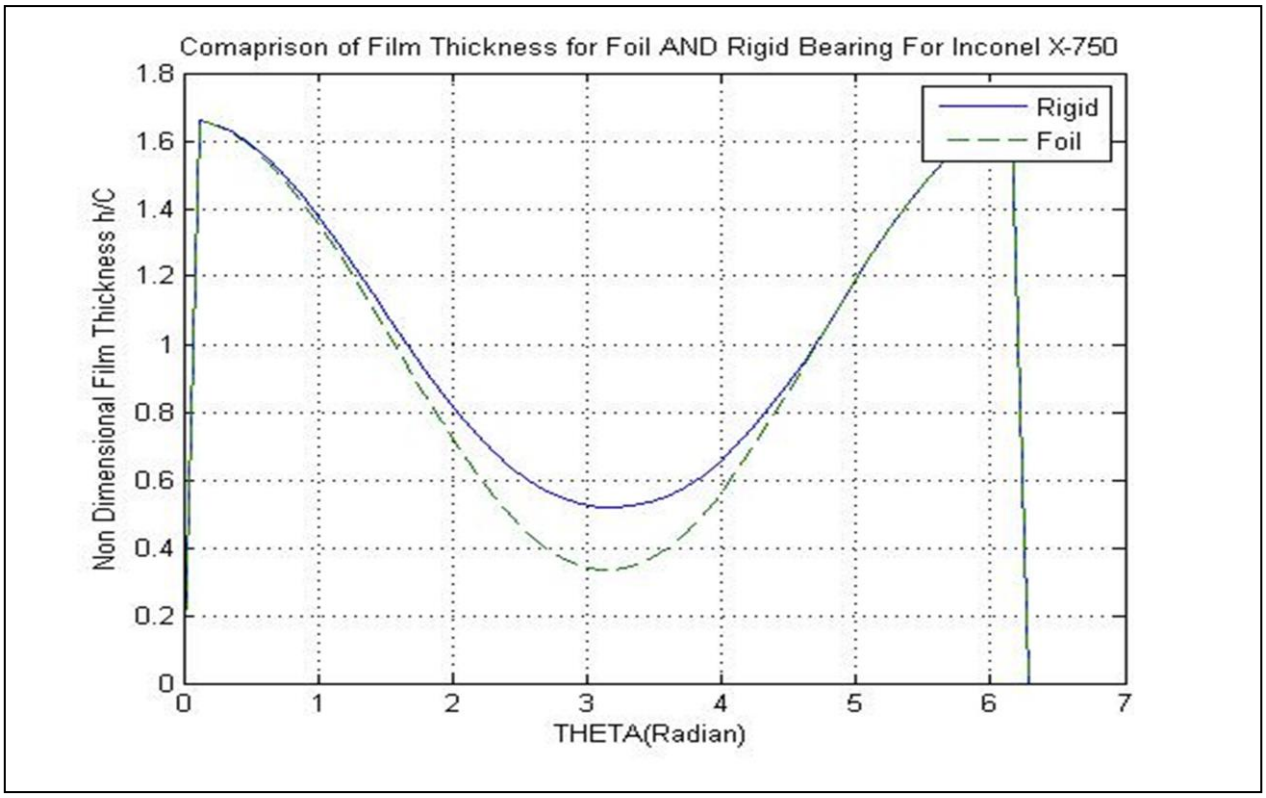

Figure 5.03: Comparison of film thickness of foil and rigid bearing for Inconel X-750

Another comparison is made between the foil and rigid bearing in terms of pressure profile.

We can see that the higher pressure is generated in case of foil bearing than is obtained in rigid bearing.

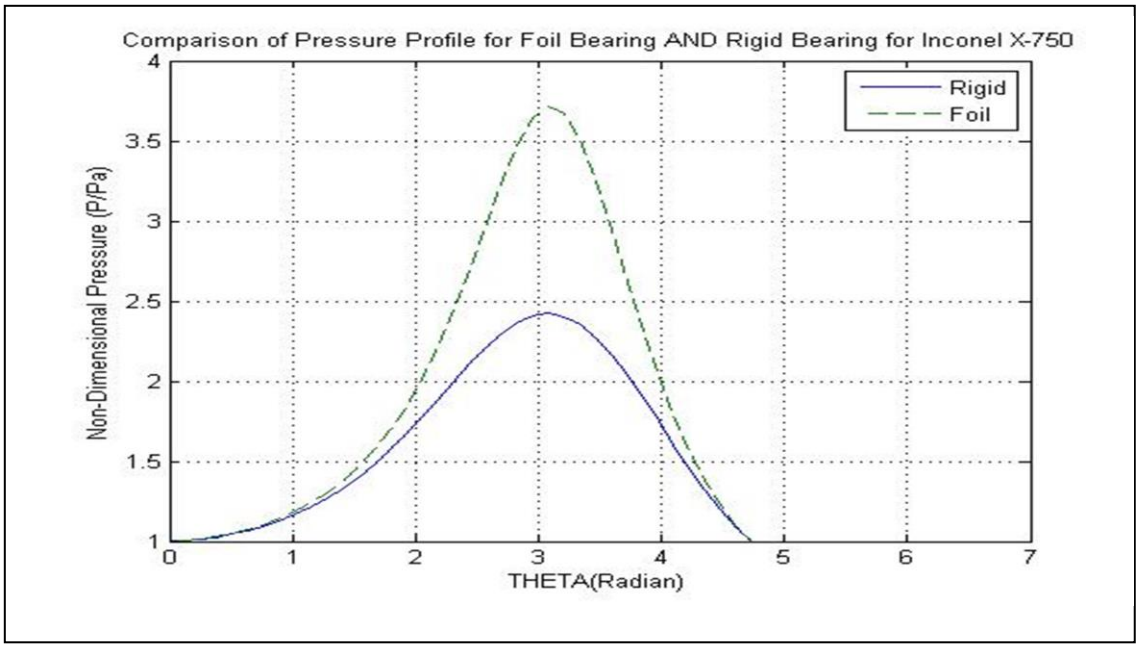

Figure 5.04: Comparison of non-dimensional pressure of foil and rigid bearing for Inconel X-750

5.1.4 Variation of Load Carrying Capacity with Eccentricity Ratio

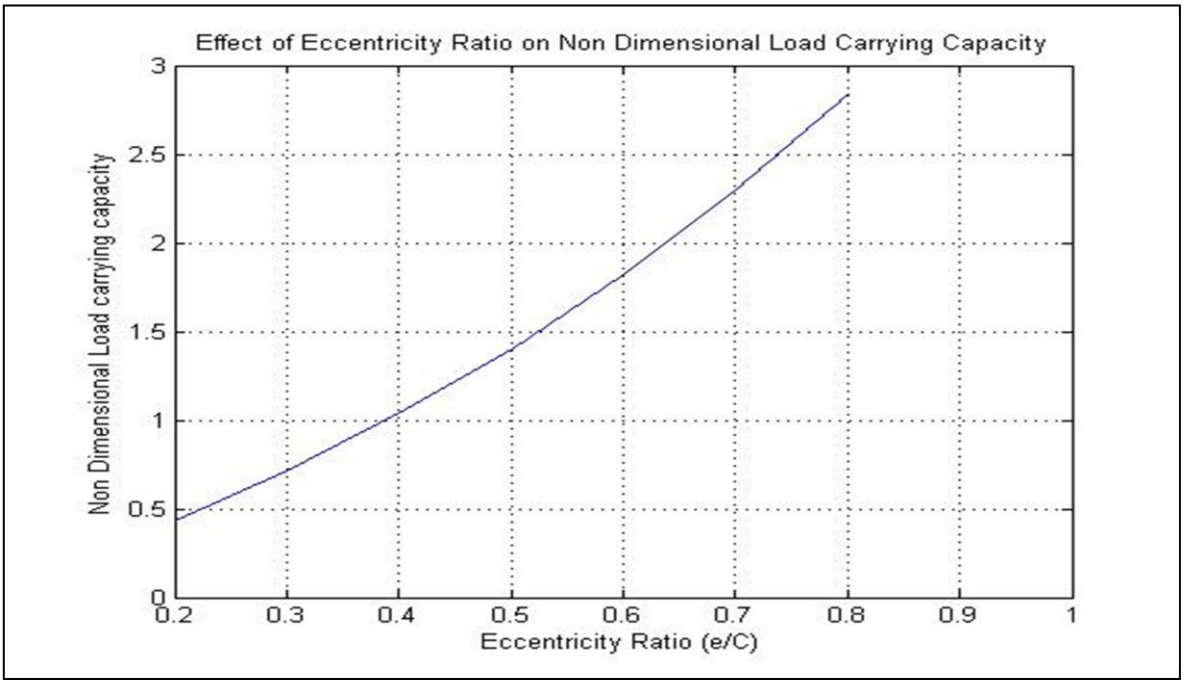

Figure 5.05: Variation Non-Dimensional Pressure with eccentricity ratio

As the eccentricity ratio is increase the load carrying capacity is also increased. But there is limitation to increase eccentricity ratio as higher eccentricity will cause larger vibration.

5.1.4 Variation of Load Carrying Capacity with Angular Speed of Rotation

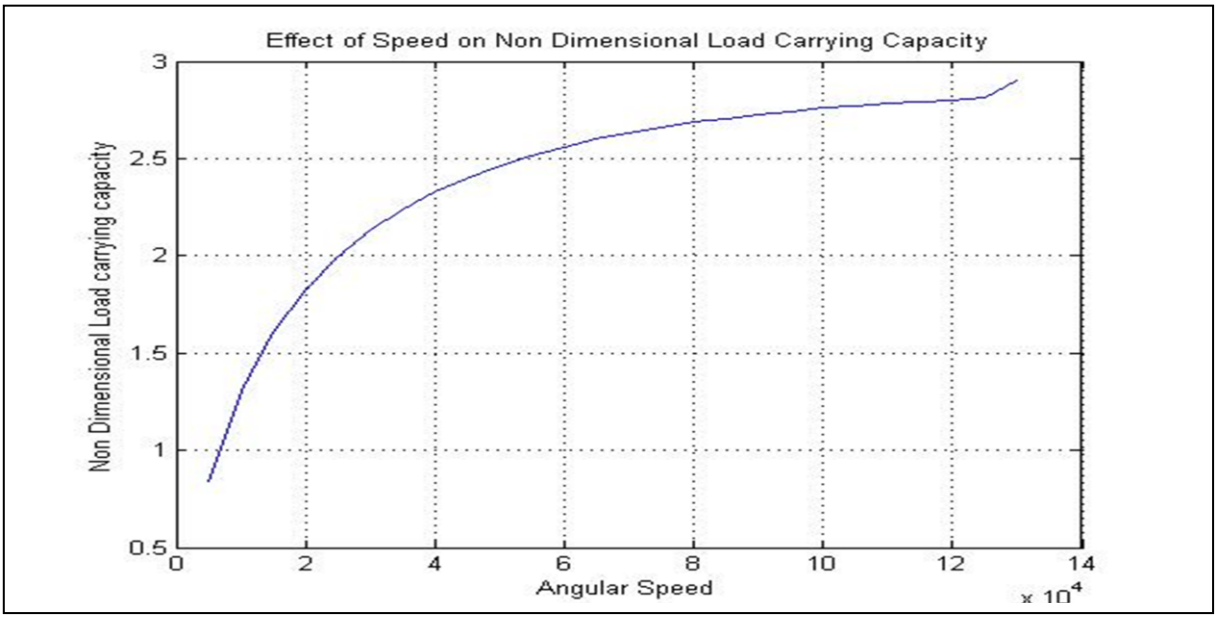

Figure 5.06: Variation of Load Carrying Capacity with Angular Speed

As we can see as the speed of rotation increases from 5000 rpm, the load carrying capacity also increases. However it becomes almost a constant after certain speed, (from 80000 rpm to 1, 30,000 rpm load carrying capacity remains a constant.

5.1 ANALYSIS OF MATERIAL OF BUMP FOIL: Aluminium Bronze

Next material to be selected was Aluminium Bronze since it is one of the bump foil materials used in manufacturing the bump foils of bearings chiefly employed in low temperature applications. Some of the areas of application of Inconel X-750 are

- Cryogenic Centres
- Refrigerator Compressors

Considering the properties of this material we give the following inputs:

Sl. No.	Input Property	Value	Unit
1.	Radial Clearance (C)	0.03	mm
2.	Radius of Shaft (R)	25	mm
3.	Length of bearing (Le)	50	mm
4.	Eccentricity (e)	0.02	mm
5.	Bump pitch (s)	3.17	mm
6.	Atmospheric Pressure (pat)	0.1	N/mm2
7.	Half Bump length (l)	1.125	mm
8.	Thickness of bump foil (t)	0.1	mm
9.	Poisson's ratio (υ)	0.34	-
10.	Viscosity of lubricant(η)	17.8*10-12	N-s/mm2
11.	Angular speed of Rotation (ω)	30000	rpm
12.	Eccentricity ratio esp. = e/C	0.67	-
13.	Modulus of Elasticity of bump foil (Et)	120000	N/mm2
14.	No. of grid points in theta direction (M)	50	-
15.	No. of grid points in zbar direction (N)	50	-
16.	No. of iterations	1000	-

Table 5.2: Input properties with Aluminium bronze as bump foil material

With the help of the above properties, the MATLAB Code is solved for certain fixed number of iterations. Aluminium Bronze has Poisson's Ratio of 0.33 and Modulus of Elasticity of 120GPa, these being the two most important mechanical properties of the bump foil material.

Similarly giving the inputs in the MATLAB Code we get the following plots for Aluminium Bronze as shown in the next pages:

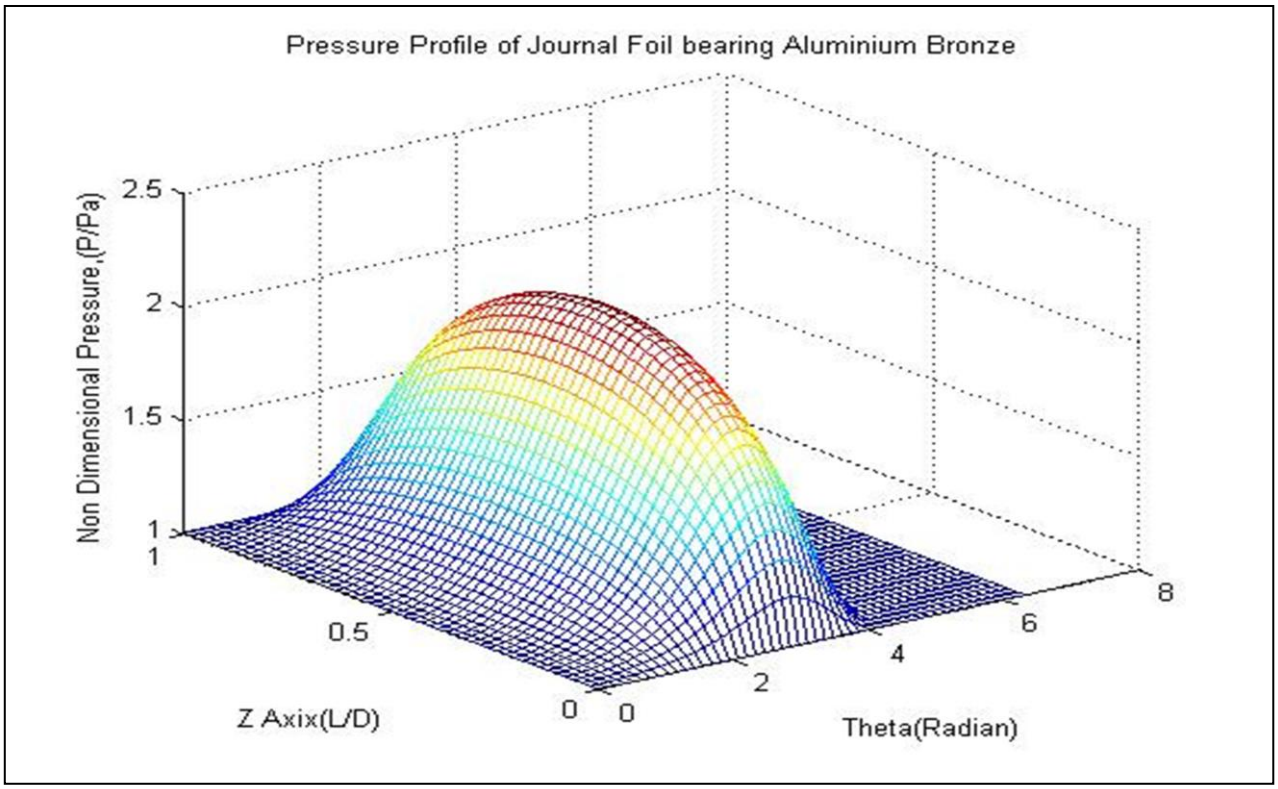

Figure 5.07: Pressure Profile of Journal Foil Bearing for Aluminium Bronze

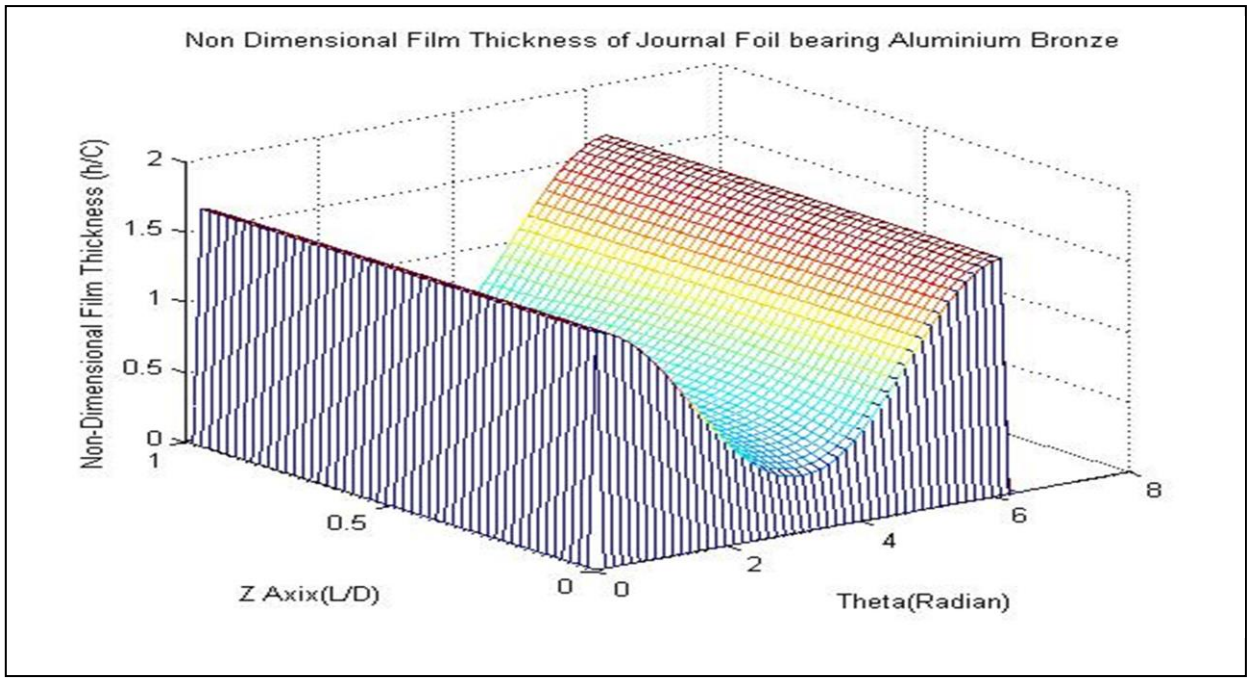

Figure 5.08: Non Dimensional Film Thickness of Journal Foil Bearing for Aluminium Bronze

Figure 5.09: Comparison of film thickness of foil and rigid bearing for Aluminium Bronze

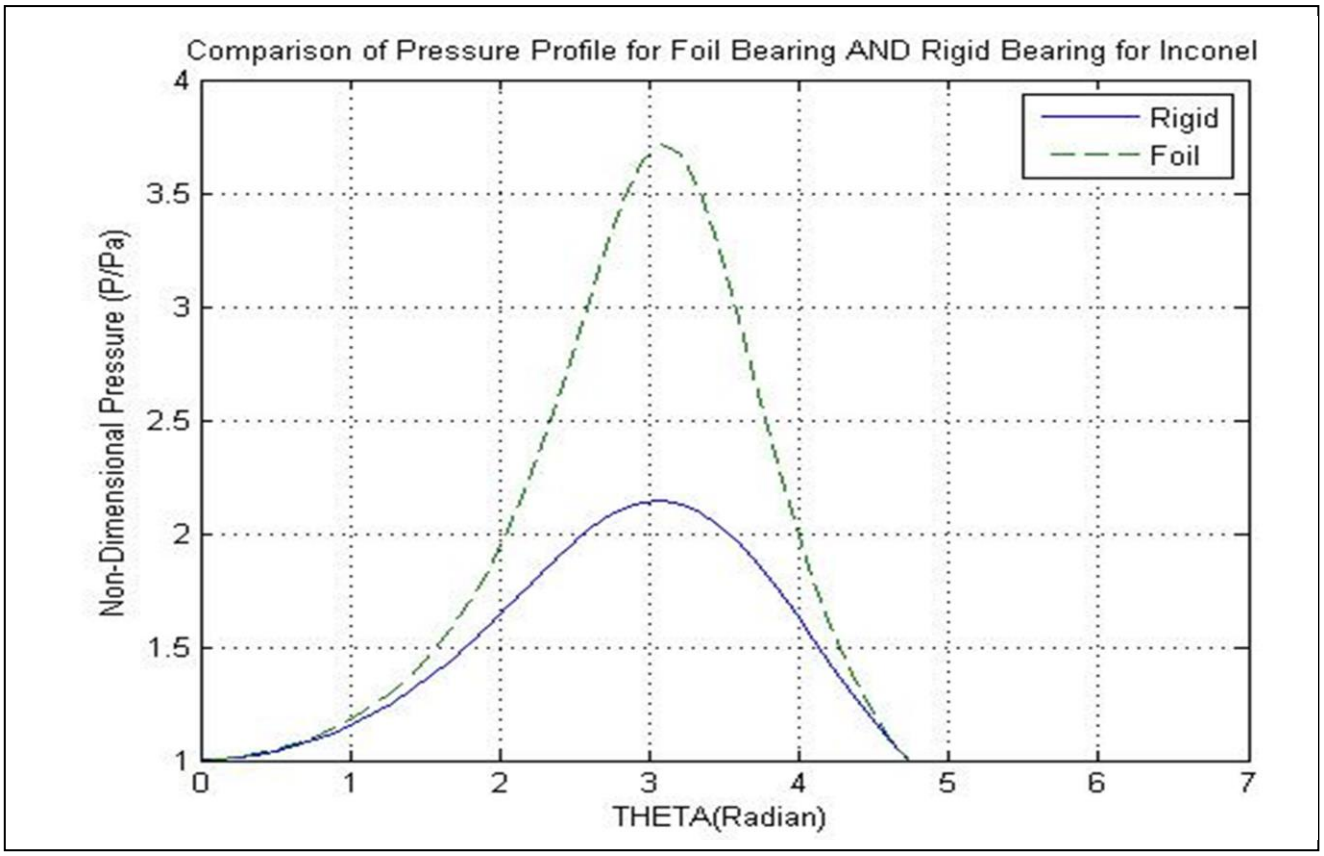

Figure 5.10: Comparison of non-dimensional pressure of foil and rigid bearing for Aluminium Bronze

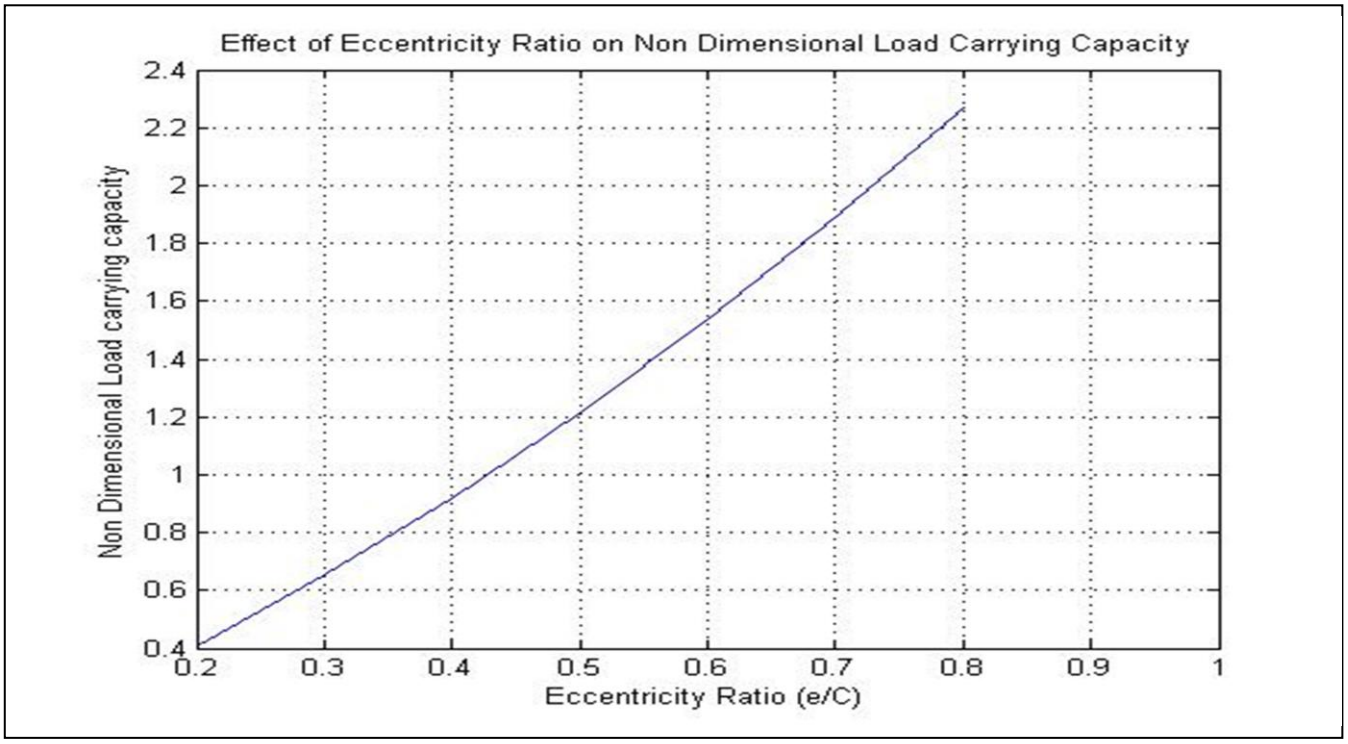

Figure 5.11: Variation of Non-Dimensional Pressure with Eccentricity Ratio

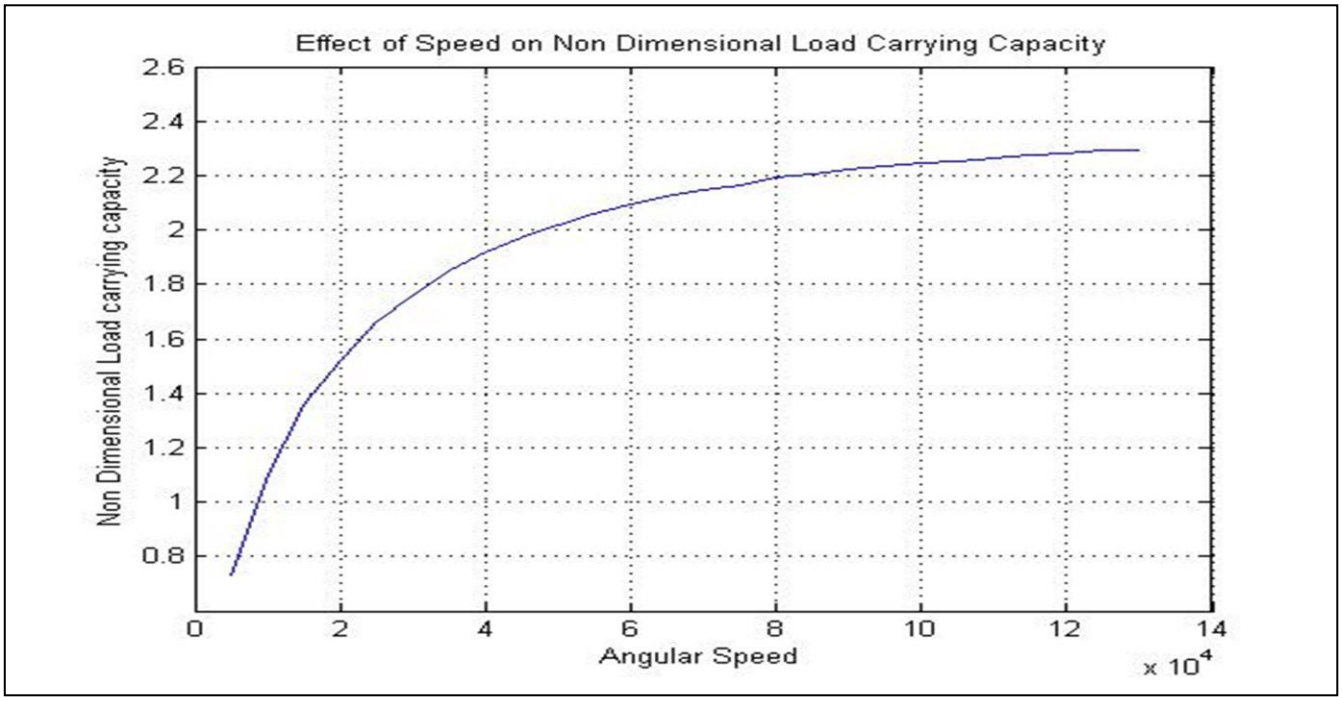

Figure 5.12: Variation of Non-Dimensional Pressure with Angular Speed

CHAPTER 5

CONCLUSIONS

The ever growing needs of the aerospace rotating machinery, microturbines and other forms of turbomachinery requires aerodynamic rather hydrodynamic analysis of the compliant foil bearings to critically analyse their operating parameters. Their main principle of operation is governed by Reynolds Equation. But to solve this non-linear partial differential equation a lot of computational time and effort is consumed. In the current project the Finite Difference Method is used to solve the Reynolds Equation. Use of non-Dimensionalization and using the method of Quadratic Solution are the unique features of this project. In the current project an attempt was made to find the performance parameters like pressure profile, film thickness, load carrying capacity etc. with several assumptions to simplify modified Reynolds equation. The analysis was performed on two types of bump foil materials:

1. Inconel X-750
2. Aluminium Bronze

Both these materials are found to be commercially used in turbines and generators etc. Due to protected (copyrighted) technology of gas foil journal bearings, very less or rather very small amount of work is found in open literatures. The results of the current project may be useful to the researchers to work more on further analysis of compliant foil journal bearings.

CHAPTER 6

FUTURE SCOPES

Although a large amount of information on the various parameters of the bearings can be predicted for any foil bearing by following through my research work but certainly there is always scope for future research both experimentally and analytically to be done on foil bearings. The following studies about bearings can be done in the near future:

- In Turbomachine laboratories various types of experimental work can be performed for firstly designing the journal foil bearings and then comparing it with the already available theoretical results.
- As already shown investigating the non dimensional load carrying capacity, one can use various optimisation algorithms to find out the various parameters like eccentricity ratio, angular speed of rotation for most efficient performance of the bearings.
- We can also look forward to finding out the temperature rise of the bearings through its thermodynamic analysis and thus improve its performance.
- There is also a scope for finding out the stiffness and damping characteristics of the journal foil bearing, thus one can have knowledge about the vibrations of the bearing.

CHAPTER 7

REFERENCES

1. **DellaCorte, Christopher R. Zaldana, Antonio C. Radil, Kevin** (2004), "A Systems Approach to the Solid Lubrication of Foil Air Bearings for Oil-Free Turbomachinery", Journal of Tribology, Vol. 126, 200-207.
2. **Morosi Stefano, IlmarF.Santos** (2011), "Active lubrication applied to radial gas journal bearings", Tribology international, Vol. 42, 1949-1958.
3. **DellaCorte, Christopher, C. Radil, Kevin, J. Bruckner, Robert, S. Adam, Howard** (2008), "Design, Fabrication, and Performance of Open Source Generation I and II Compliant Hydrodynamic Gas Foil Bearings" , Tribology Transactions, 51:3, 254-264
4. **D. Kim, S.Park**, (2009), "A Preliminary study of the load bearing capacity of a new foil thrust gas bearing", Tribology International42 (2009) 413–425
5. **Arora V., Hoogt P. J. M. van der, Aarts R.G.K.M., De Boer A.Der**, (2010), "Identification of dynamic properties of radial air-foil bearings", DOI 10.1007/s10999-010-9137-z
6. **Howard Samuel A., Dykas Brian,** (2004), "Journal Design Considerations for Turbomachine Shafts Supported on Foil Air Bearings", Tribology Transactions, 47: 508-516, 2004
7. **Dellacorte C., Valco M. J.**, (2000), "Load Capacity Estimation of Foil Air Journal Bearings for Oil-Free Turbomachinery Applications", Tribology Transactions, 43: 795-801, 2000
8. **Kumar Manish, Daejong Kim**, (2010), "Static performance of hydrostatic air bump foil bearing", Tribology International 43(2010)752–758
9. **Zywica Grzegorz**, (2011), "The Static performance analysis of the foil bearing structure", Acta mechanica et automatica, vol.5 no. 4
10. **Daejong Kim, Soongook Park** (2009), "Hydrostatic Air foil bearings, Analytical and experimental Investigation", Tribology International 42(2009)413-425
11. **Lee Y.B., Kim T.H., Kim C.H**. (2004), "Unbalance Response of a Super Critical Rotor supported by Foil Bearings-Comparison with test results", Tribology Transactions 47:54-60, 2004

12. **Hoy Yu, Chen Shuangtao, Zhang Qiaoyu, Zhao Hongli**, (2011), ”Numerical study on foil journal bearings with protuberant foil structure”, Tribology International, 44(2011)1061-1070
13. **Dong-Hyun Lee, Young Cheol Kim, Kyung Woong Kim**, (2010), “The effect of Coulomb friction on the static performance of foil journal bearings”, Tribology International, 43(2010) 1065-1072
14. **Santiago Oscar De, Andres Luis San**, (2011), “Parametric Study of Bump Foil Gas Bearings for Industrial Applications”, Proceedings of ASME Turbo Expo 2011, Canada
15. **Feng Kai, Kaneko Shigehiko**, (2010), “Parametric studies on static performance and non linear instability of bump type foil bearings”, Journals of System Design and Dynamics, Vol.4 No.6, 2010.
16. **Reddy Amith Hanumappa**, (2005), “Hydrodynamic Analysis of Compliant Journal Bearings”, Thesis for the degree of Master of Science, Lousiana State University
17. **Chengchun Peng**, (2003),”Thermodynamic Analysis of Compressible Gas Flow in Compliant Foil Bearings”, Thesis for the degree of Master of Science, Louisiana State University.

ROAD MAP

Work done in 7th Semester

Schedule of work	Aug-12	Sep-12	Oct-12	Nov-12	Status
Literature survey					Completed
Derivation of Reynolds equation for Thrust bearings					Completed
Compressible Reynolds Equation in Two Dimensions					Completed
Finite difference analysis of 2D equations					Completed

Work done in 8th Semester

Schedule of work	Jan-13	Feb-13	Mar-13	Apr-13	Status
Finite difference analysis of 2D equations					Completed
Writing program in MATLAB					Completed
Results and Discussions					Completed